



Review

Advances in bioorganic molecules inspired degradation and surface modifications on Mg and its alloys

Lei Cai^{a,1}, Di Mei^{b,1}, Zhao-Qi Zhang^b, Yuan-ding Huang^c, Lan-Yue Cui^a, Shao-Kang Guan^{b,*}, Dong-Chu Chen^d, M. Bobby Kannan^{e,f}, Yu-feng Zheng^g, Rong-Chang Zeng^{a,b,h,**}

^aCorrosion Laboratory for Light Metals, College of Materials Science and Engineering, Shandong University of Science and Technology, Qingdao 266590, China

^bSchool of Materials Science and Engineering, Zhengzhou University, Zhengzhou 450002, China

^cMagIC - Magnesium Innovation Centre and Institute of Metallic Biomaterials, Helmholtz-Zentrum Hereon, Max-Planck Straße 1, Geesthacht 21502, Germany

^dSchool of Materials Science and Energy Engineering, Foshan University, Foshan 528000, China

^eSchool of Engineering, University of Newcastle, Callaghan, NSW 2308, Australia

^fCollege of Science and Engineering, James Cook University, Townsville, QL 4811, Australia

^gSchool of Materials Science and Engineering, Peking University, Beijing 100871, China

^hHubei Key Laboratory of Advanced Technology for Automotive Components, Wuhan University of Technology, Wuhan 430070, China

Received 16 October 2021; received in revised form 12 December 2021; accepted 9 February 2022

Available online 7 March 2022

Abstract

Mg alloys possess biodegradability, suitable mechanical properties, and biocompatibility, which make them possible to be used as biodegradable implants. However, the uncontrollable degradation of Mg alloys limits their general applications. In addition to the factors from the metallic materials themselves, like alloy compositions, heat treatment process and microstructure, some external factors, relating to the test/service environment, also affect the degradation rate of Mg alloys, such as inorganic salts, bioorganic small molecules, bioorganic macromolecules. The influence of bioorganic molecules on Mg corrosion and its protection has attracted more and more attentions. In this work, the cutting-edge advances in the influence of bioorganic molecules (i.e., protein, glucose, amino acids, vitamins and polypeptide) and their coupling effect on Mg degradation and the formation of protection coatings were reviewed. The research orientations of biomedical Mg alloys in exploring degradation mechanisms *in vitro* were proposed, and the impact of bioorganic molecules on the protective approaches were also explored.

© 2022 Chongqing University. Publishing services provided by Elsevier B.V. on behalf of KeAi Communications Co. Ltd.

This is an open access article under the CC BY-NC-ND license (<http://creativecommons.org/licenses/by-nc-nd/4.0/>)

Peer review under responsibility of Chongqing University

Key words: Magnesium alloy; Biomaterial; Bioorganic molecules; Degradation; Coating; Glucose.

1. Introduction

Magnesium (Mg) alloys exhibit light weight, high specific strength [1], good electromagnetic shielding performance and shock resistance, biocompatibility and biodegradability as well [2–4], which have wide application prospects in 3C products, automotive, high-speed rail, and aerospace together with biomedical fields [5,6]. Their biocompatibility and biodegradability make them possible to be used as biodegradable metallic materials. Mg is a constant element in human body, which can activate a variety of enzymes, participates in human

* Corresponding author.

** Corresponding author at: Corrosion Laboratory for Light Metals, College of Materials Science and Engineering, Shandong University of Science and Technology, Qingdao 266590, China.

E-mail addresses: skguan@zsu.edu.cn (S.-K. Guan), rczeng@foxmail.com (R.-C. Zeng).

¹ These authors contributed equally to this work.

metabolic processes, promotes the absorption of calcium, and thus promotes bone growth [7,8]. The excessive Mg^{2+} ions produced by the dissolution of implanted Mg can be excreted via body fluid metabolism process, and do not lead to toxic reaction [9,10]. Mg could be completely degraded *in vivo*. However, its standard electrode potential is as low as -2.37 V vs. standard hydrogen electrode (SHE). Thus, hydrogen depolarization corrosion of Mg is prone to occur [11,12]. In addition, the comparable mechanical properties (i.e., elastic modulus) of Mg alloys to natural bone reduces stress shielding effect greatly [13]. Based on the relevant advantages of Mg alloys, scientists and engineers currently focus their interests on Mg-based bone fixation implants and vascular stents [3,14–19].

However, the relatively rapid and uncontrollable degradation limits the development and general applications of Mg and its alloys. The aggressive Cl^- ions in body fluids have a significant effect on Mg corrosion [20]. Excessive corrosion of Mg leads to the premature failure of the implants, which cannot achieve the original intention of treatment. Once the rapid degradation of Mg-based materials initiates, hydrogen bubbles will be probably formed, which disturb the healing process of the surrounding tissues [21–23]. Besides, the localized alkaline micro-environment caused by the degradation process is also potentially harmful for the surrounding tissues [24].

It is of great importance to study the degradation behavior of Mg alloys. The research on Mg degradation for biomedical applications is inevitably related to the simulation of service body fluid environment. The influence of inorganic salts on Mg degradation has been firstly valued [25–28]. However, the body fluids in human body contain both inorganic ions and various organic molecules, which may have different impacts on the service of Mg implants. For instance, Witte et al. [21] once demonstrated that the degradation rate *in vitro* is not significantly consistent with that *in vivo*. This finding may be partially attributed to the influence of bioorganic molecules. Therefore, scientists have explored the role of bioorganic molecules, such as protein [29–35], lipids [36,37], monosaccharides (i.e., glucose) [38–42], amino acids [43–45] and vitamins [46], on Mg corrosion. However, due to complex human environment and the fluids with various components, the individual effect of a simple organic substance on Mg corrosion is insignificant. Therefore, the synergetic effects of different organic molecules on Mg corrosion have been explored. This provides more theoretical insights into the understanding on the degradation behavior of Mg alloys as biodegradable implants during service period.

In this review, the cutting-edge progresses in bioorganic molecules-related corrosion on Mg is introduced. The research characteristics and future research outlooks are proposed.

2. Influencing factors on MG alloy corrosion

The influencing factors on Mg degradation are shown in Fig. 1. From the metallic material perspective, alloy ele-

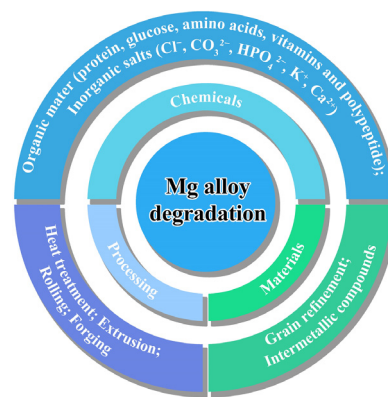


Fig. 1. Influencing factors regarding the degradation of Mg alloys.

ments [47–49], microstructure [50–52], and heat treatment [48,53–55] and processing [53,56–59] as well affect the anti-corrosion property of Mg alloys markedly [60,61].

The micro-environment around Mg sample during corrosion process is mainly affected by solution pH value [62], aggressive ions, and temperature, among which the corrosive medium is one of the most significant factors. For instance, the service environment of vascular stent and blood vessel, is very complicated, including (1) inorganic salt ions, such as Cl^- [27,63–65], CO_3^{2-} [26,63,64], HPO_4^{2-} [27,64,66], K^+ , Ca^{2+} [63], (2) organic compounds, such as protein, glucose, amino acids, and (3) gases, such as oxygen and carbon dioxide, together with water, which constitute the complex microenvironment of human body. All these factors exert remarkable effect on corrosion of Mg alloys.

2.1. Influence of inorganic ions

There are many kinds of inorganic salts in body fluids, which not only maintain the stability of pH value and osmotic pressure, but also participate in a series of life activities. As an important anion in human body, Cl^- ions have been proven to have the acceleration effect on Mg corrosion [67–69]. Cl^- has strong electronegativity and takes the advantage when competing with OH^- and other ions for cations, so it affects the stability of $Mg(OH)_2$ products. It has a critical influence on the localized corrosion of Mg alloys [20,26,70]. $H_2PO_4^-/HPO_4^{2-}$ and CO_2/HCO_3^- play a pH-buffered role in the human body. Phosphates, resulted from $H_2PO_4^-/HPO_4^{2-}$, inhibit Mg degradation markedly. Carbonate leads to the dissolution of Mg, but also promotes the rapid passivation of Mg surface via the formation of carbonate precipitation. All the mentioned reactions are shown in Fig. 2.

Just as above-mentioned, HCO_3^- , $H_2PO_4^-$ and HPO_4^{2-} ions can react with Mg^{2+} ions, leading to an insoluble protective layer on Mg surface so as to alleviate Mg corrosion [64]. Ca^{2+} ion reacts with phosphate/carbonate, giving rise to precipitates, which also delays the corrosion of the matrix. Other cations, such as Na^+ and K^+ , almost remain steady in body fluid and their effects on Mg corrosion of Mg alloys have scarcely been noticed.

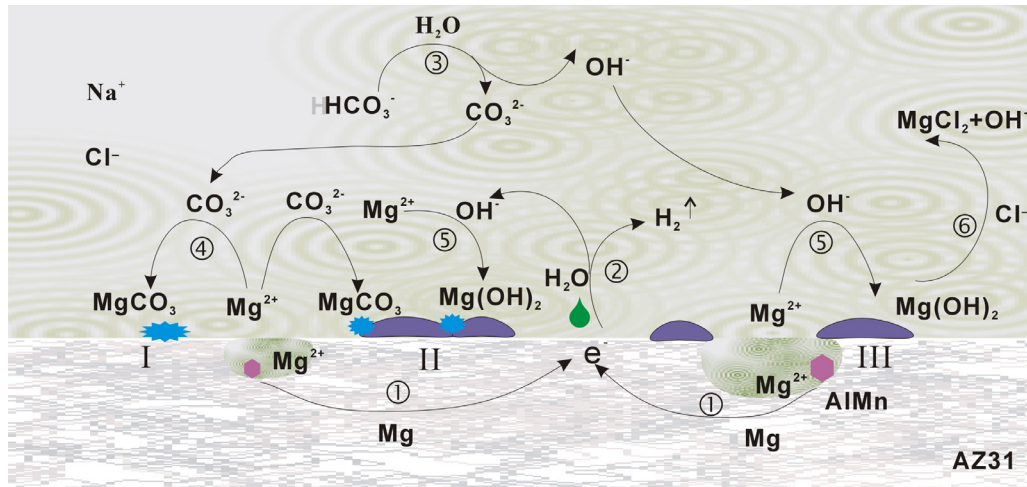


Fig. 2. Formation mechanism of bicarbonates during the corrosion of magnesium alloy AZ31 [25]. (Reproduced with permission of Ref [25]. Copyright of © 2014 Elsevier).

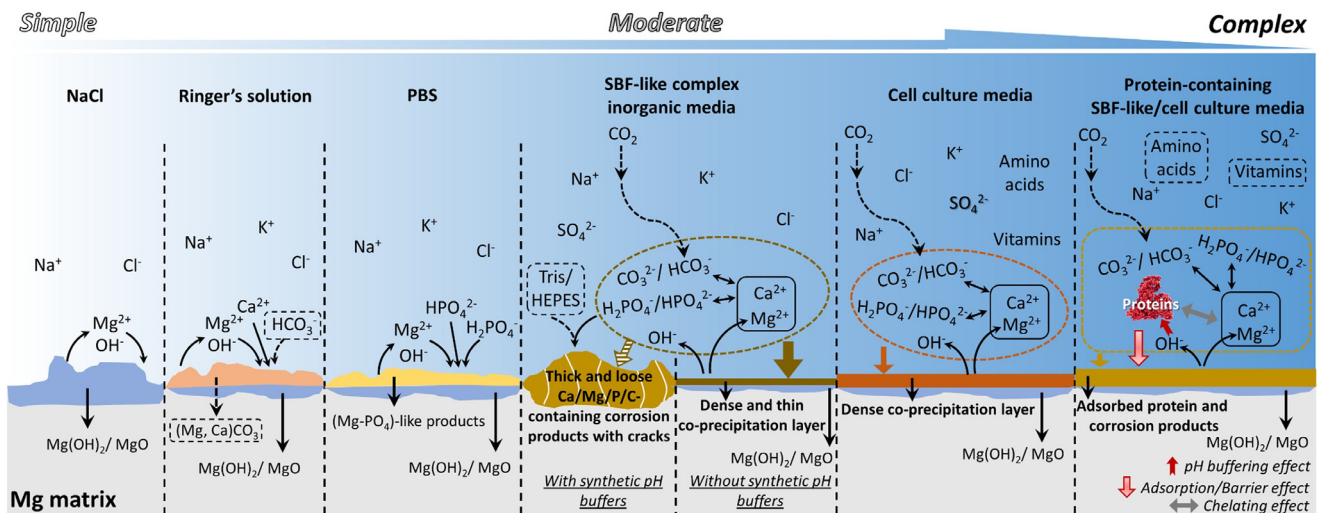
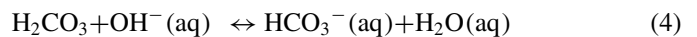
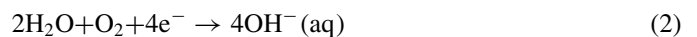
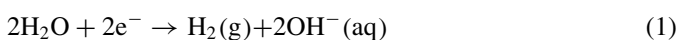


Fig. 3. Corrosion mechanisms of Mg in different media [71]. (Reproduced with permission of Ref [71]. Copyright of © 2020 Elsevier).

Fig. 3 shows several corrosion mechanisms are responsible for the corresponding corrosion when immersion in different corrosion media, including NaCl, Ringer's solution, PBS, SBF-like complex inorganic media, cell culture media and SBF-like/cell culture media with protein addition.

2.2. Influence of gas

When the living body is exchanging gas, hemoglobin combines with O_2 , and then CO_2 releases, so a part of O_2 and CO_2 are dissolved in the body fluid. Normally, hydrogen evolution reaction Eq. (1) was normally believed as the cathode reaction in corrosion of Mg. In recent years, the role of oxygen reduction or oxygen consumption reaction has received increasing attention in the cathode reactions of Mg corrosion (Eq. (2)) [72–76]. Carbon dioxide is combined with Mg^{2+} in the form of HCO_3^- or CO_3^{2-} (Eq. (3) and ((4) [25].



2.3. Influence of organic compounds

The proteins, glucose, amino acids, vitamins and other organic substances in body fluids play a major role in participating in life activities and providing energy for life activities. It is, thus, necessary for focusing the influence of organic molecules or compounds on Mg degradation [30,38,77]. It is of such a great importance to investigate their effects on Mg corrosion that scientists can take insight into understanding the service performance of Mg implants. In the following

sections, the effects of bioorganic molecules on Mg corrosion are introduced.

3. Influence of bioorganic molecules on corrosion

3.1. Influence of protein

Protein is the main undertaker of life activities, with structural diversity and functional diversity. After implantation, the surface of the implant firstly contacts with the blood and tissue in human body so that the protein is adsorbed on the Mg surface to form an adsorption layer, which not only affects the coagulation, cell and bacterial adhesion of metal surface, but also significantly influences the corrosion of metal materials [29–31]. The structure of proteins [78], the surface state of substrates and the condition of media [79–81] play a significant role in the protein adsorption. Some relevant results showed that the protein can accelerate or inhibit Mg corrosion in the various electrolytes [32–34,82,83]. In our previous work, adsorption, chelating and pH buffering of protein were recognized as three main aspects that affect Mg corrosion in protein-containing electrolytes [84]. Different test environment ultimately affects the adsorption mechanism of proteins on Mg corrosion.

The effects of bovine serum on the degradation behavior of pure Mg has been explored by Hou et al. [77]. The results showed that the organic molecules remarkably influenced the degradation rate of pure Mg by altering the formation of corrosion product layer. The influence of albumin on the degradation behavior of Mg-Ca alloy was observed *in situ* by Liu [11]. The results designated that the adsorption of albumin molecules on sample surface results in the decrease in corrosion rate and the inhibition of Cl^- induced filiform corrosion. Albumin at higher concentration showed more obvious inhibition efficiency on Mg filiform corrosion.

The chemical composition of alloys also affects the proteins adsorption. Wang et al. [85] employed molecular dynamics (MD) simulation and experimental methods to investigate the effects of eight alloying elements, such as Ca, Li, Ce, Y, Zr, Mn, Zn and Cu, on the adsorption behavior of fibrinogen C-terminal fragment on Mg surface. The results showed that Ca and Ce promote the adsorption of fibrinogen significantly, whereas, Mg and Cu exhibit an opposite effect. It was also found that the second phases or intermetallic compounds also influence on the adsorption of fibrinogen. Fibrinogen is preferentially adsorbed on the intermetallic compounds that contain Y-, Ce-, or Nd-, instead of Zn- [86].

Hou et al. [87] compared the degradation behavior of Mg in simulated body fluid in the presence of bovine serum albumin (BSA) and fetal bovine serum (FBS) under different flow conditions. It was found that both BSA and FBS possessed minor inhibition effect on Mg corrosion in Hanks' solution under static conditions due to the formation of protein adsorption layer and Ca-P-rich products. Under dynamic flow conditions, BSA and FBS showed an opposite effect (Fig. 4). It could be attributed to that the flow rate weakened the ad-

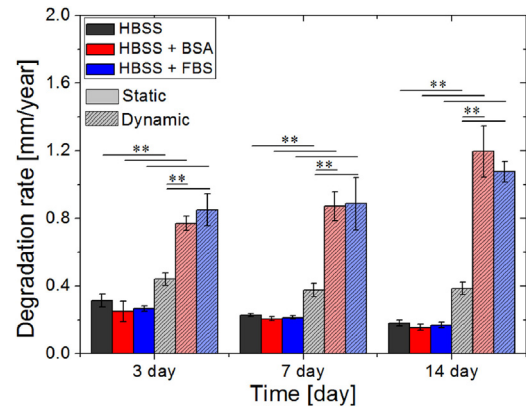


Fig. 4. Degradation rate of pure Mg in different solutions under different flow conditions. (Significance level: (**): $p < 0.01$) [87]. (Reproduced with permission of Ref [87]. Copyright of © 2021 Elsevier).

sorption effect and the adhesion between Ca-P products and Mg substrate.

Computer simulation methods are beneficial for deeper understanding about how protein participates in the corrosion reaction of Mg alloys. Zhang et al. [88] employed molecular dynamic (MD) simulation and experimental analysis to explore the adsorption behavior of BSA on the micro-arc oxidation (MAO) coated Mg surface. The results showed that the negatively charged O atoms of BSA interact with and the dissolved Mg^{2+} and ionically adsorbed on Mg surface. The MD simulation results indicated that MAO processed ability to capture BSA via the MgO on the MAO coating.

3.2. Influence of enzymes

Enzymes are proteins with high specificity and high catalytic efficiency. Zhang et al. [89] found pepsin slowed down the corrosion rate of Mg wires in simulated gastric fluid (SGF), while pancreatin accelerated Mg corrosion in simulated intestinal fluid (SIF). Both of them affect Mg corrosion by altering the corrosion products layer on sample surface. The adsorption of pepsin inhibits the pitting corrosion of Mg wires in SGF. However, pancreatin destroys the integrity of the products film (MgHPO_4), resulting in relatively uneven degradation of Mg wires, as shown in Fig. 5.

3.3. Influence of glucose

Saccharides are important organic compounds widely distributed in nature. They are the main source of energy needed by all living bodies to maintain life activities. In particular, a higher glucose level in human body means diabetes. When Mg implant was used in the blood vessel of diabetic, glucose level is an important factor that affect Mg corrosion. Zeng et al. [38] firstly paid attention on the influence of glucose and its coupling with amino acids or protein on Mg degradation. It was found that the increase of glucose content in normal saline leads to the rapid corrosion of pure Mg due to rapid conversion of glucose to gluconic acid, which at-

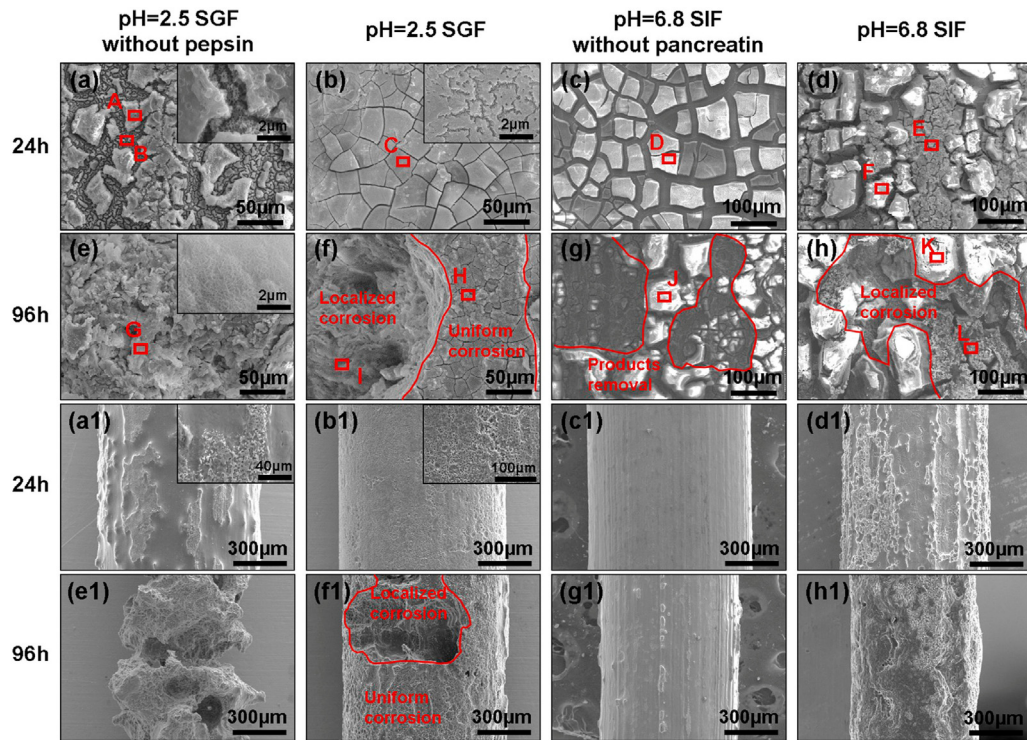


Fig. 5. Corrosion morphology of Mg wires after immersion in different SGF and SIF [89]. (Reproduced with permission of Ref [89]. Copyright of © 2022 Elsevier).

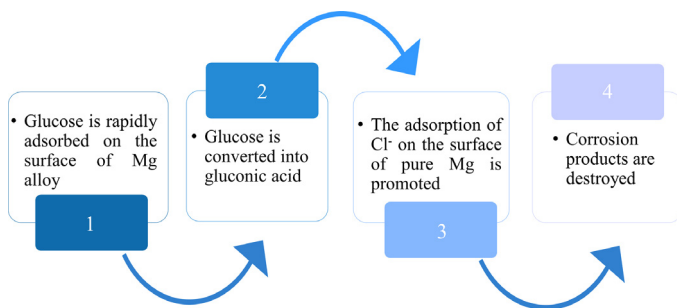
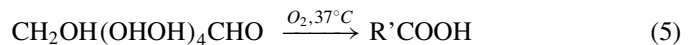


Fig. 6. Role of glucose molecules in pure Mg corrosion in saline (0.9% NaCl).

tacks corrosion products and leads to the lower pH of the solution. At the same time, chloride ions are more preferentially adsorbed on Mg surface, also resulting in the increase of corrosion rate (Fig. 6). In Hanks' solution, the increase of glucose content promotes the formation of calcium phosphate (Ca-P) compounds on Mg surface, then resulting in the higher corrosion resistance. This finding provides a new strategy for the preparation of Ca-P coating using glucose. This novel Ca-P coating has been successfully fabricated by Zeng's group and will be introduced in later section.

The corrosion mechanism of pure Mg in glucose-containing electrolytes is proposed as follows: firstly, the aldehyde (-CHO) group of glucose is activated and is oxidized to gluconic acid. The comparison between glucose and mannitol shows that the aldehyde group of glucose becomes the carboxyl (-COOH) group (Fig. 7), and the formed -COOH is the

main factor for the aggravation of corrosion. Reaction equations are shown in Eqs. (5) and (6). In addition, the strong adsorption and adhesion ability of glucose result in Cl^- enrichment. Therefore, the synergistic attack of the retained Cl^- and gluconic acid leads to the expansion of the cracks on $\text{Mg}(\text{OH})_2$ products and provides a way reach the matrix, thus improving the dissolution activity (Fig. 8).



Li et al. [40] explored the coupling effect of glucose and Tris on the corrosion behavior of AZ31 Mg alloy. 6.118 g/L Tris was added into 0.9% NaCl solution to investigate the effect of glucose with different content (0–3 g/L) on Mg corrosion. It showed that the increase of glucose contents accelerates Mg corrosion in Tris-buffered 0.9% NaCl solution (Fig. 9). For the influence of glucose on the corrosion fatigue (CF) of Mg alloys, Liu et al. [41] found that the higher content of glucose increased the corrosion resistance and CF of Mg alloy in Hank's solution.

Besides for Mg alloys, glucose also shows a great impact on the corrosion behavior of other biodegradable metallic materials. Liu et al. [90] investigated the corrosion performance of zinc alloys in glucose-containing environment. It is shown that glucose significantly affected the biodegradation of zinc by accelerating the formation of biodegradation products.

There are a number of studies focused on the roles of glucose, but less studies take care the effects of other monosac-

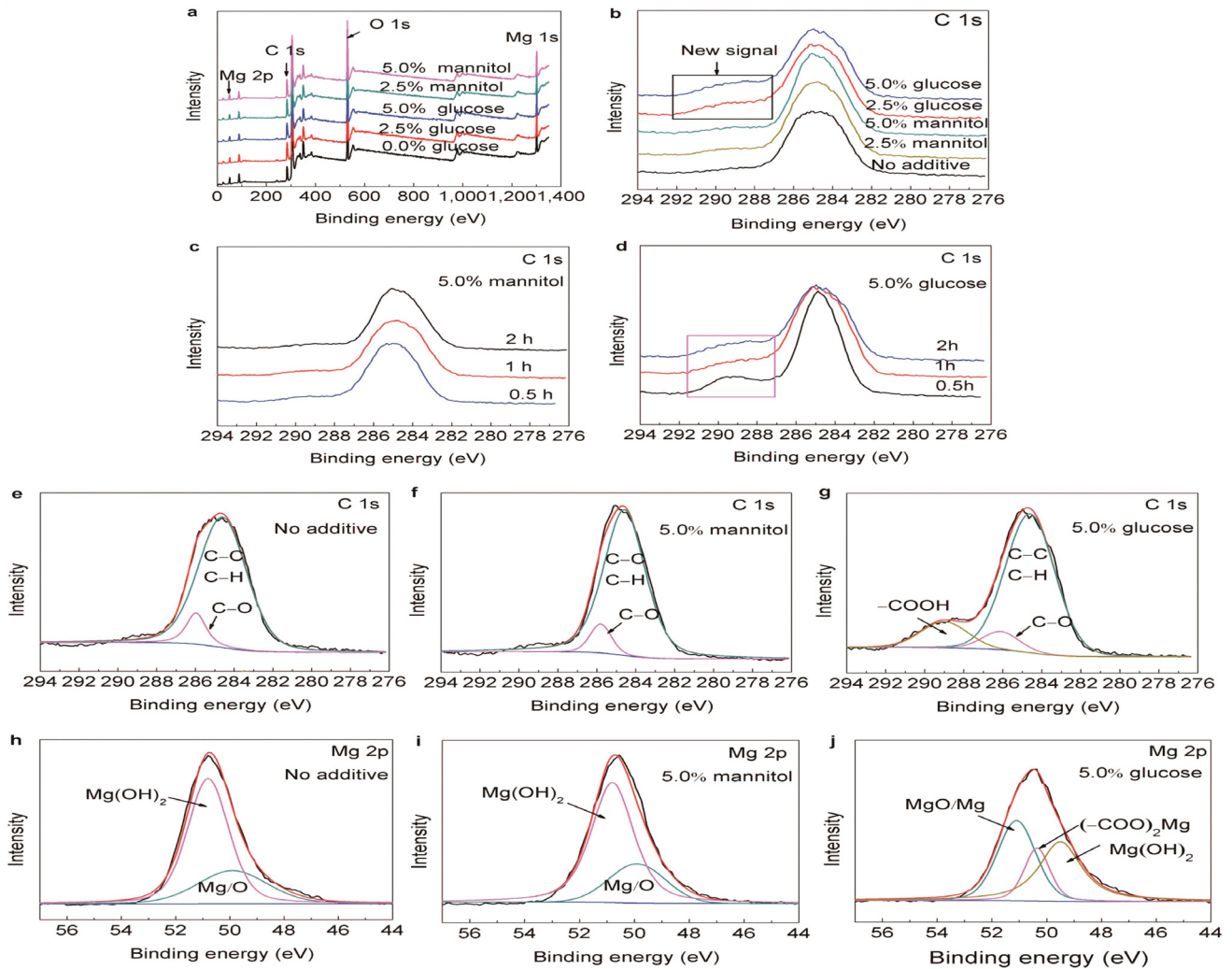


Fig. 7. XPS analysis of corroded pure Mg after soaking in saline solution (in absence and presence of glucose or mannitol for different times. The entire range (a) and C 1 s spectra (b) for corroded surfaces in glucose-containing NaCl solutions for 2 h (c,d) C 1 s spectra of corroded samples mannitol-containing NaCl solutions (c) and with glucose (d) for different time. Curve fitting of C 1 s spectra (e–g) and Mg 2 p spectra (h–j) for the samples immersed in different solutions for 2 h [38]. (Reproduced with permission of Ref [38]. Copyright of © 2015 Nature publishing group).

charides on the *in vitro* degradation of Mg alloys. Pokharel et al. [42] found that D-fructose promoted the deposition of phosphate, formed the thick and dense corrosion products, and inhibited Mg corrosion in simulate body fluid. Mei et al. [46] determined the effects of four monosaccharides (glucose, galactose, glucosamine, and fructose) on the corrosion rate of Mg-0.8Ca and pure Mg. It is found that glucosamine led to the rapid corrosion of Mg-0.8Ca in SBF and NaCl. Its acceleration efficiency in SBF is inferior to that in NaCl solution. The effect of abovementioned four saccharides on pure Mg in NaCl solution is relatively low, which is consistent with the negligible individual effect of four saccharides. However, the mixed saccharides led to an accelerated corrosion for pure Mg due to the complex reaction between the glucosamine and Ca^{2+} in SBF.

Table 1 summarizes the effects of different content of glucose on the degradation of different alloys in different test environments. It could be found that the degradation of Mg alloy in 0.9 wt.% NaCl is accelerated with the increase of

glucose content. In Hanks'-like solutions, the increase of glucose content inhibits Mg degradation. Therefore, it could be concluded that the effect of glucose on the Mg degradation depends on the type of saccharides, the type of test media and the added content.

3.4. Influence of amino acids

Among the 20 basic amino acids of human body, nine amino acids are essential for human body. According to the polarity of side chain groups, they can be categorized into non-polar amino acids and polar amino acids (polar neutral, acidic and basic amino acids) as shown as Fig. 10. According to the chemical structure, they can also be divided into aliphatic, aromatic, and heterocyclic amino acids.

More than 40 years ago, amino acid compounds were firstly used as corrosion inhibitors for metallic materials. Amino acid is a kind of safe corrosion inhibitor, which is

Table 1
Effect of glucose on corrosion of Mg alloy.

Alloy type	Monosaccharide type	Concentration	Corrosive medium	Other additives	Corrosion rate	Refs.
Pure Mg	Glucose	0%, 2.5%, 5.0%	0.9%NaCl	Null	0%<2.5%<5.0%	[38]
Pure Mg	Glucose	1 g/L, 2 g/L, 3 g/L	Hanks'	Null	3 g/L<2 g/L<1 g/L	
Mg-1.35Ca	Glucose	0 g/L, 25 g/L, 50 g/L	0.9%NaCl	Null	0%<2.5%<5.0%	[39]
AZ31	Glucose	0 g/L,1 g/L, 2 g/L,3 g/L	0.9%NaCl	6.1181 g/L (50.5 mM) Tris	1 g/L<0 g/L<2 g/L<3 g/L Tris +0 g/L<Tris +1 g/L<Tris +2 g/L<Tris +3 g/L Glu<Glu+ Tris 3 g/L<1 g/L	[40]
Mg-Zn-Zr-Y	Glucose	1 g/L,3 g/L	Hank s'	Null	3 g/L<1 g/L	[41]
AZ31	D-fructose	1 g/L	SBF	Null	Decelerated	[42]
Pure Mg	Glucose	5.83×10^{-3} M	0.9%NaCl	Null	Accelerated	[46]
Mg-0.8Ca	Glucose	5.83×10^{-3} M	0.9%NaCl	Null	Accelerated	[46]
Pure Mg	Galactose	1.11×10^{-3} M	0.9%NaCl	Null	Decelerated	[46]
Mg-0.8Ca	Galactose	1.11×10^{-3} M	0.9%NaCl	Null	Accelerated	[46]
Pure Mg	Glucosamine	4.97×10^{-3} M	0.9%NaCl	Null	Accelerated	[46]
Mg-0.8Ca	Glucosamine	4.97×10^{-3} M	0.9%NaCl	Null	Accelerated	[46]
Pure Mg	Fructose	4.44×10^{-4} M	0.9%NaCl	Null	Decelerated	[46]
Mg-0.8Ca	Fructose	4.44×10^{-4} M	0.9%NaCl	Null	Accelerated	[46]
Pure Mg	Glucose,	5.83×10^{-3} M	0.9%NaCl	Null	Decelerated	[46]
Mg-0.8Ca	galactose,	1.11×10^{-3} M	0.9%NaCl	Null	Accelerated	[46]
Pure Mg	glucosamine	4.97×10^{-3} M	SBF	Null	Accelerated	[46]
Mg-0.8Ca	and fructose	4.44×10^{-4} M	SBF	Null	Decelerated	[46]

Table 2
Individual and group effects of vitamins on the corrosion performance of Mg-0.8Ca and CP Mg [46].

Vitamins	Concentration/M	Medium	Mg-0.8Ca	CP Mg
Ascorbic acid (VC)	1.14×10^{-4}	0.9%NaCl	Accelerated	Decelerated
Folic acid (VB9)	2.27×10^{-6}	0.9%NaCl	Accelerated	Decelerated
Inositol (VB8)	3.89×10^{-5}	0.9%NaCl	Accelerated	Accelerated
Riboflavin (VB2)	2.66×10^{-7}	0.9%NaCl	Accelerated	Decelerated
Pyridoxine-HCl (VB6)	4.82×10^{-6}	0.9%NaCl	Accelerated	Decelerated
Thiamine- HCl (VB1)	2.96×10^{-6}	0.9%NaCl	Decelerated	Decelerated
Nicotinamide (VB3)	8.19×10^{-6}	0.9%NaCl	Accelerated	Accelerated
Choline chloride (VB4)	7.16×10^{-6}	0.9%NaCl	Decelerated	Accelerated
Calcium pantothenate (VB5)	2.10×10^{-6}	0.9%NaCl	Accelerated	Accelerated
All above listed vitamins tested together		0.9%NaCl	Accelerated	Decelerated
		SBF	Decelerated	Decelerated

environmentally friendly, nontoxic, biodegradable, and relatively cheap [91,92].

L-methionine has been used as a corrosion inhibitor for low carbon steel in sulfuric acid [93]. Eddy [94] investigated three kinds of amino acids as corrosion inhibitors for mild steel. The results indicated that the inhibition efficiency of amino acids is related to the type of heteroatom in their chemical structure, and the order of inhibition ability of oxygen, nitrogen and sulfur is $S > O > N$. In addition, it was found that inhibitory effect of straight chain amino acids was weaker than that of branched chain amino acids. For the amino acids with different aromatic rings, a good corrosion inhibition performance owing to the presence of electron donor groups on the ring.

Amino acids have also been tried to use as corrosion inhibitors for Mg alloys. Wang et al [43,44]. studied the effects

of alanine, glutamic acid, lysine and L-cysteine on the corrosion mechanism of pure Mg. The results showed that alanine, glutamic acid and lysine inhibited Mg corrosion. The order of inhibition effect was alanine, glutamic acid and lysine. Amino acid molecules could react with Mg ion and phosphate ion to form different Mg phosphate precipitates on the surface of the matrix, which can inhibit the further corrosion of matrix. The reaction was related to the length of the carbon chain of amino acid. The shorter the carbon chain, the easier the reaction. When pure Mg was immersed in PBS solution, polarized $-NH_2$ could promote the formation of phosphate. Finally, phosphate aggregates to form clusters (Fig. 11). L-cysteine also inhibit the degradation of pure Mg. There is an amino group and a carboxyl group in the structure of L-cysteine, which is negative in saline solution due to the higher pH value of the solution than the isoelectric point of

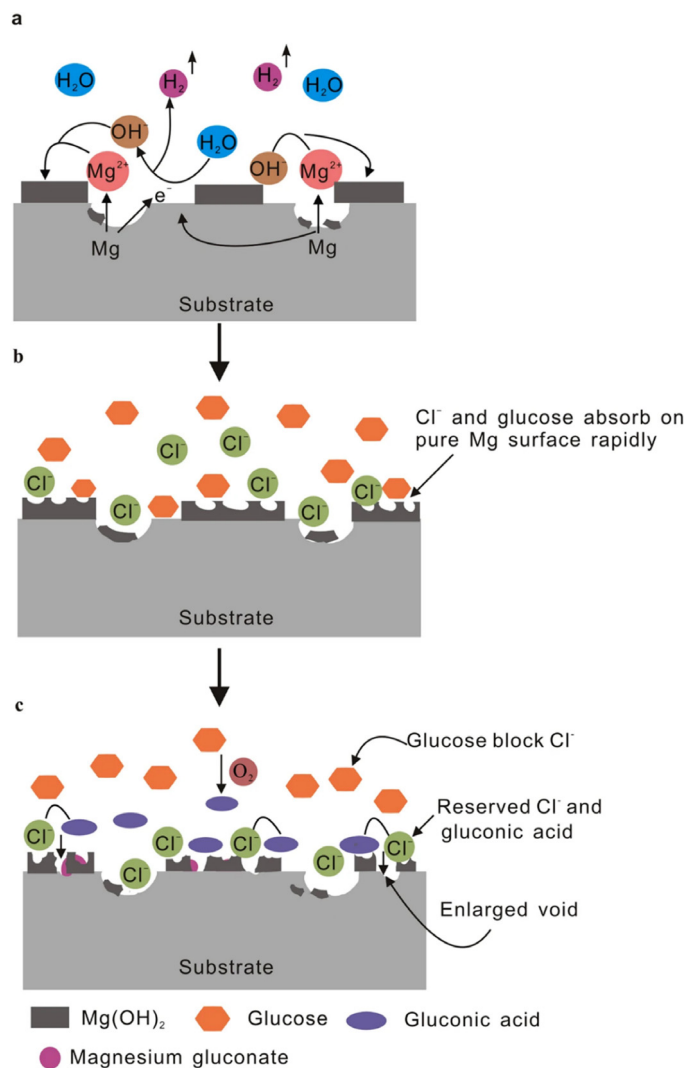


Fig. 8. Schematic illustration of the degradation process of pure Mg in glucose-containing NaCl solution [38]. (Reproduced with permission of Ref [38]. Copyright of © 2015 Nature publishing group).

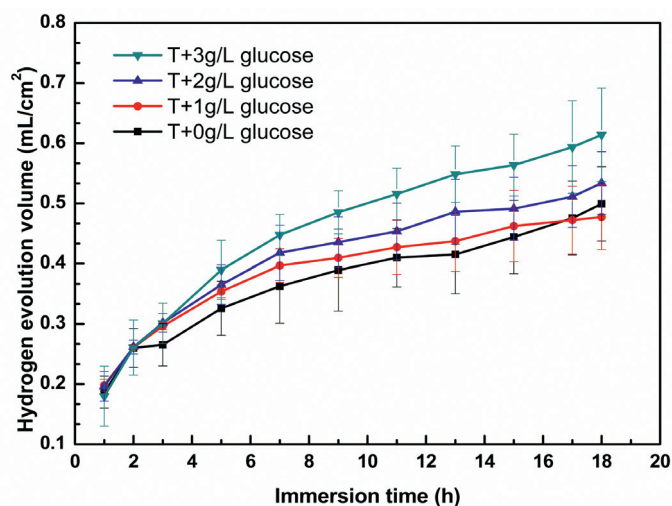


Fig. 9. Hydrogen evolution curve of AZ31 alloy in Tris-buffered saline solutions with different glucose contents [40]. (Reproduced with permission of Ref [40]. Copyright of © 2018 SpringerLink).

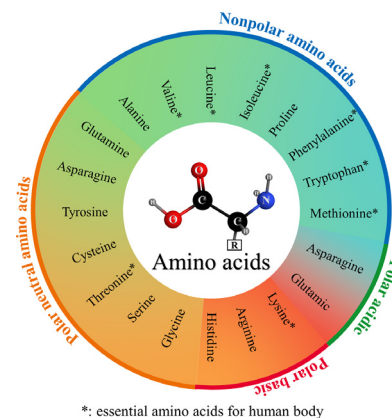
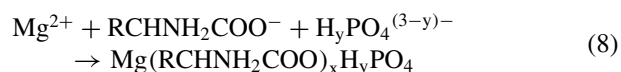
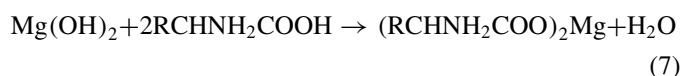


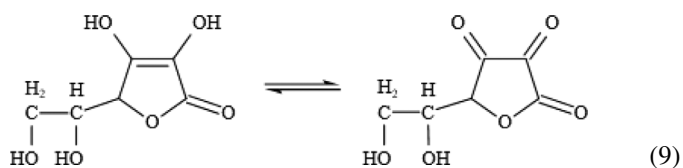
Fig. 10. Types of the amino acids.

cysteine (5.02). Therefore, L-cysteine molecule may combine with Mg²⁺ and be adsorbed on the sample surface to retard further corrosion Eqs. (7) and (8). Durga et al. [45] found that glycine in Hank's solution initially inhibited the corrosion of Mg alloy AZ31, but promoted the corrosion of AZ31 during the long period.



3.5. Influence of vitamins

There are few reports about the effect of vitamins on Mg corrosion. Mei et al. [46] investigated the influence of 9 kinds of vitamins, including ascorbic acid and 8 kinds of different B vitamins, on Mg corrosion. The related results are shown in Table 2. The 9 tested vitamins have minor individual and cumulative effect on Mg corrosion in NaCl and SBF solutions due to the low tested concentration. Studies have shown that 0.05 M VB9 and VC solution have strong corrosion inhibition effect on several Mg alloys including commercial pure Mg (CP Mg). The crystal of ascorbic acid is very stable in air, but the solution of ascorbic acid is rapidly air-oxidized, and gradually decomposes into dehydro-ascorbic acid. It further decomposes into L-threonic acid and oxalic acid in the solution over pH 4.0, as shown in Eq. (9) and (10) [95], and react with Mg afterwards. However, the studies on the effect of vitamins on Mg degradation are insufficient, especially their influencing mechanisms are worthy of further investigations.



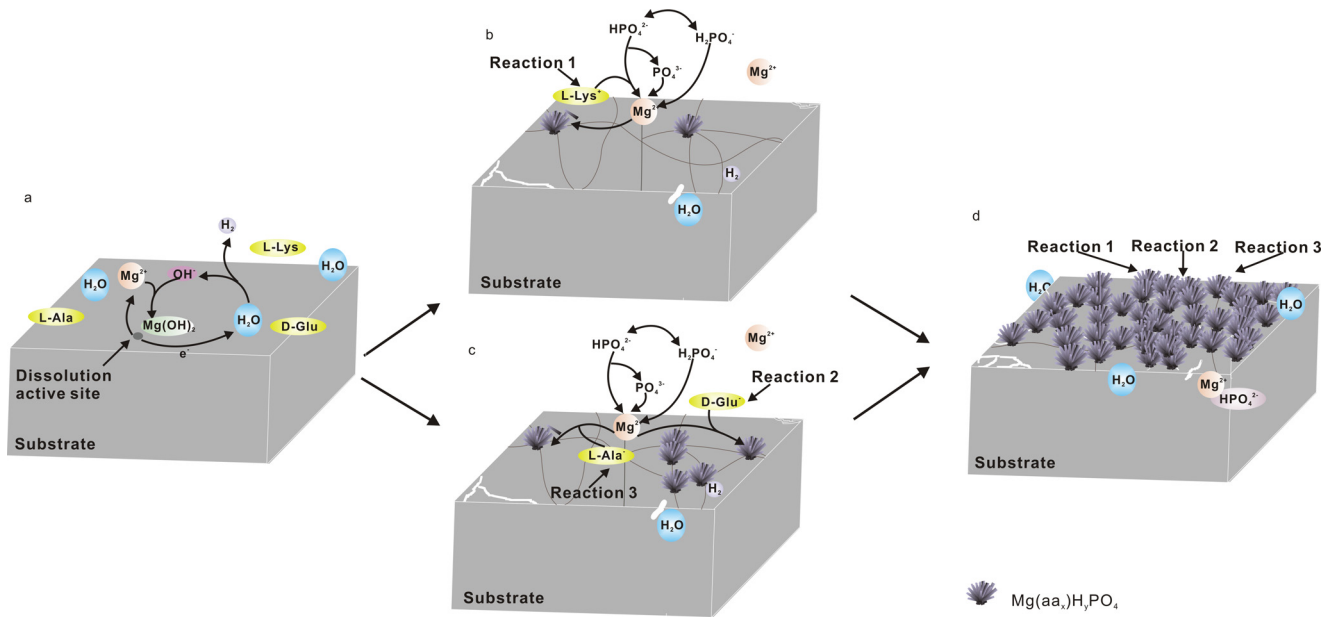
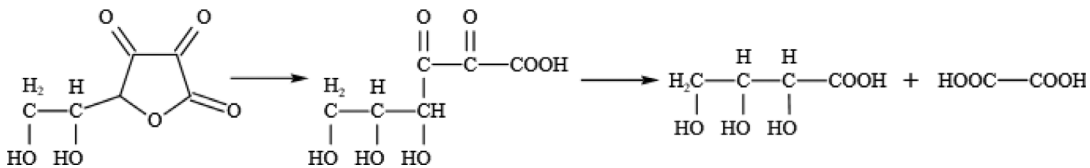


Fig. 11. Schematic illustration of the corrosion process of pure Mg in amino acid-containing PBS solutions [43]. (Reproduced with permission of Ref [43]. Copyright of © 2019 Elsevier).



(10)

4. Coupling effect of bioorganic molecules

There are many organic small molecules in the human body. The coupling of glucose and amino acid [44], glucose and protein [96] leads to the formation of new substances such as Schiff base (-C=N-) bonding between amino acid and glucose, which have different effects on Mg degradation. For instance, glucose facilitates the albumin adsorption on Mg [96]. It is necessary to understand the degradation behavior of Mg alloys under the coupling effect between bioorganic molecules.

4.1. Coupling effect of E-MEM and FBS

Yamamoto et al. [26] examined the effects of media composition on Mg degradation by 14 days' immersion test in four pseudo-physiological solutions. The degradation rate of pure Mg is greatly affected media compositions. The degradation rate in NaCl is highest, followed by that in E-MEM and Earle's solutions, and the lowest corrosion rate showed in E-MEM + FBS (Fig. 12). These results indicated that the adsorption of protein and the formation of insoluble salts prevented Mg corrosion, whereas, the organic compounds (such as amino acids) promotes the dissolution of Mg. The synthetic pH buffer, N-2-hydroxyethylpiperazine-

N'-2-ethane sulfonic acid (HEPES), accelerated Mg corrosion in NaCl, but CO₂/NaHCO₃ buffer showed opposite effect. It could be concluded that it is critical to use a suitable simulated body fluid to perform *in vitro* evaluation of Mg degradation.

4.2. The coupling effect of glucose and amino acids

Wang et al. [44] investigated the degradation mechanism of pure Mg under the combined action of L-cysteine and glucose. The co-addition of L-cysteine and glucose accelerated Mg corrosion. Previous studies [44] have shown that Schiff base (-C=N-) may be the reactant of the condensation of -NH₂ with -COH, as shown in Eq. (11). The reaction was as follows:



where, R and R' denote aliphatic and aromatic groups, respectively. It is well-known that amino acids and glucose contain R-NH₂ and R'-COH groups, respectively. Hereby, the protonation of the Schiff base group can make the molecules in acidic solution positively charged. Nitrogen atoms may deprotonate in alkaline solution and then react with Mg²⁺. As a result, the degradation of Mg was accelerated.

Fig. 13 shows the change of hydrogen evolution rate of pure Mg in aqueous solutions containing amino acids

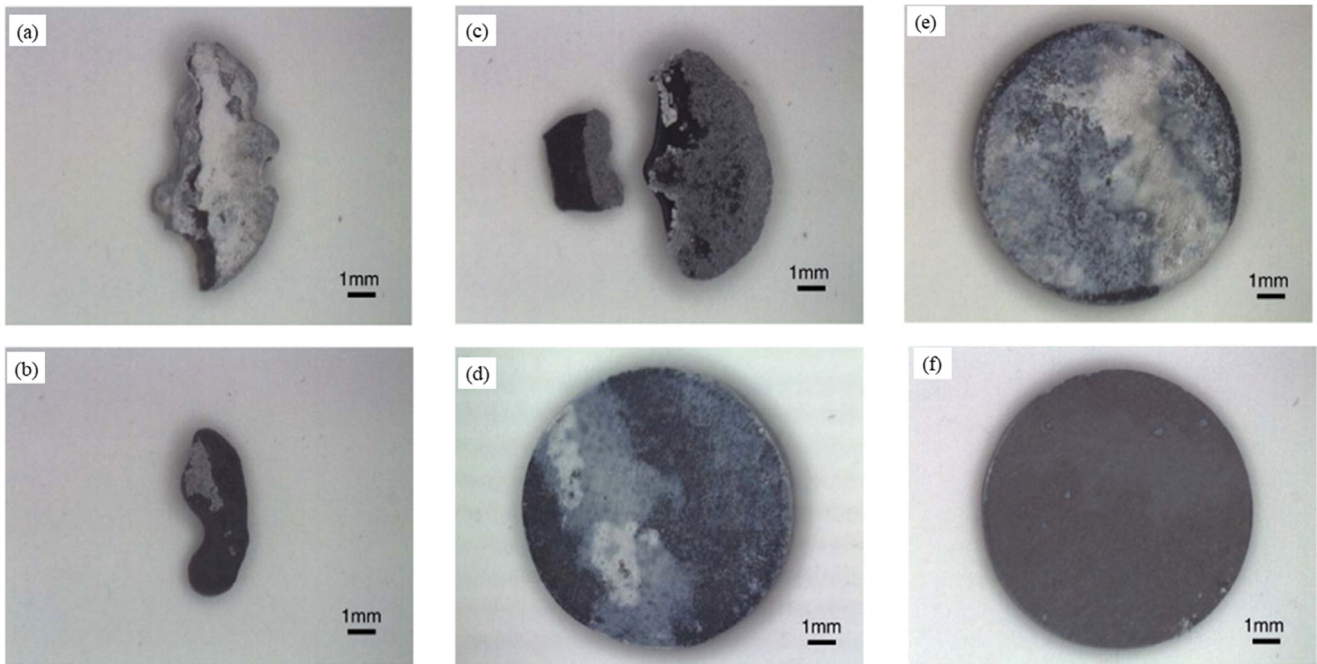


Fig. 12. Microscopic images of Mg samples after immersion in different solutions for 14 d (a) NaCl, (b) NaCl+HEPES, (c) NaCl+NaHCO₃, (d) Earle(+), (e) E-MEM, and (f) E-MEM+FBS [26]. (Reproduced with permission of Ref [26]. Copyright of © 2009 Elsevier).

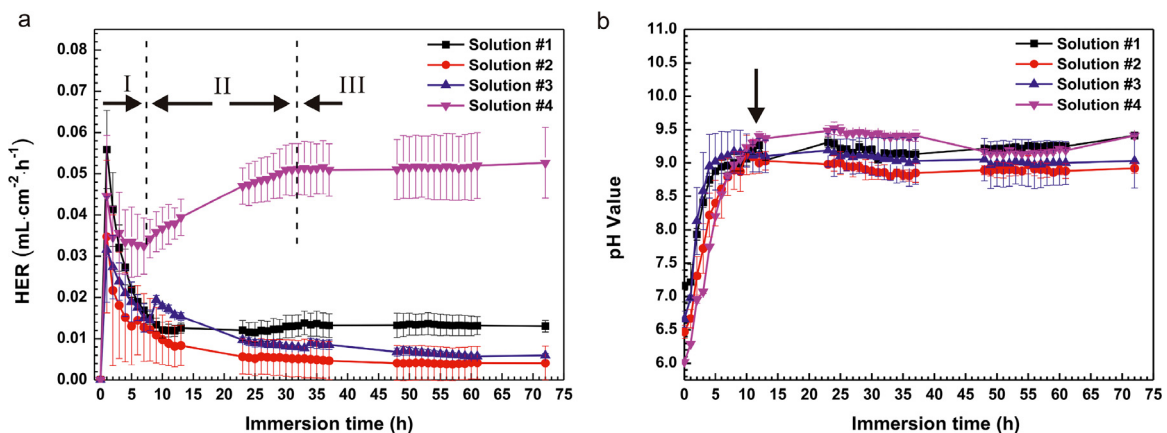


Fig. 13. (a) Hydrogen evolution rate (HER) and (b) pH curve during 72-h soaking in different solutions. (Solution #1: 0.9 wt.% NaCl; Solution #2: 0.9 wt.% NaCl + L-cysteine; Solution #3: 0.9 wt.% NaCl + Glucose; Solution #4: 0.9 wt.% NaCl + L-cysteine + Glucose) [44]. (Reproduced with permission of Ref [44]. Copyright of © 2017 MDPI).

and glucose and pH value of the media. At the first stage (Figs. 13a and 14a) of immersion period, the solution pH is lowest (Fig. 13b). In the acidic solution (pH<6.0), the accelerated dissolution of pure Mg occurs. At the stage II (soaking for 8–32 h; Figs. 13a and 14b), the alkaline solution provides the necessary conditions for the novel product formation of Schiff base, which is produced by the reaction between L-cysteine and glucose. The amount of Schiff base increases over time, and the negatively charged molecules chelate with Mg²⁺. Therefore, the Mg(OH)₂ protective film hardly precipitates on the surface. The action of Schiff base and chloride ion increased degradation rate. At the third stage (after soaking for 32 h, Fig. 14c), the corrosion rate is gradually stabilized owing to the depletion of amino acids. The formation

of Schiff bases in the hybrid solution of amino and glucose indicates the promise for the preparation of coatings on Mg alloys using amino acids and glucose.

4.3. The coupling effect of glucose and protein

Yan et al. [96] found that the low concentration of glucose (2 g/L) restrained the degradation process of Mg alloy due to the adsorption effect of glucose on Mg surface. At the later stage of immersion, protein reacted with the degradation product on Mg surface and then accelerated Mg corrosion. When glucose and protein were present simultaneously, Mg degradation was significantly suppressed and the degradation rate significantly reduced. The effects of glucose (2 g/L, 20 g/L)

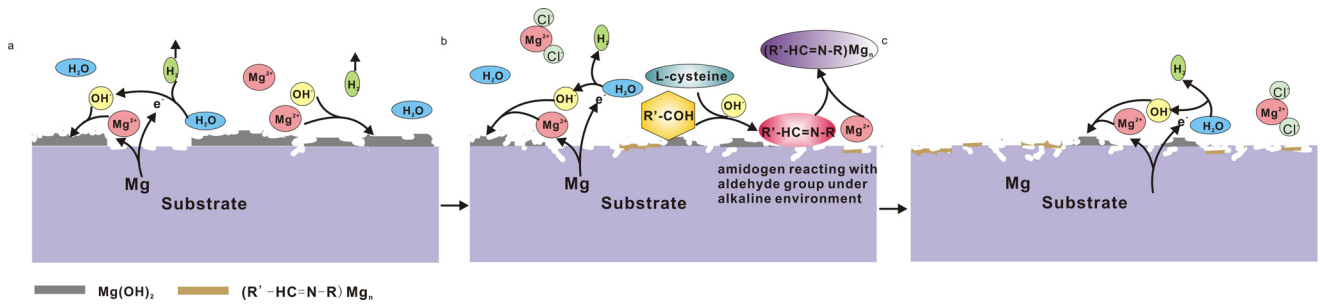


Fig. 14. Schematic diagram of the corrosion process of pure Mg in a solution containing L-cysteine and glucose [44]. (Reproduced with permission of Ref [44]. Copyright of © 2017 MDPI).

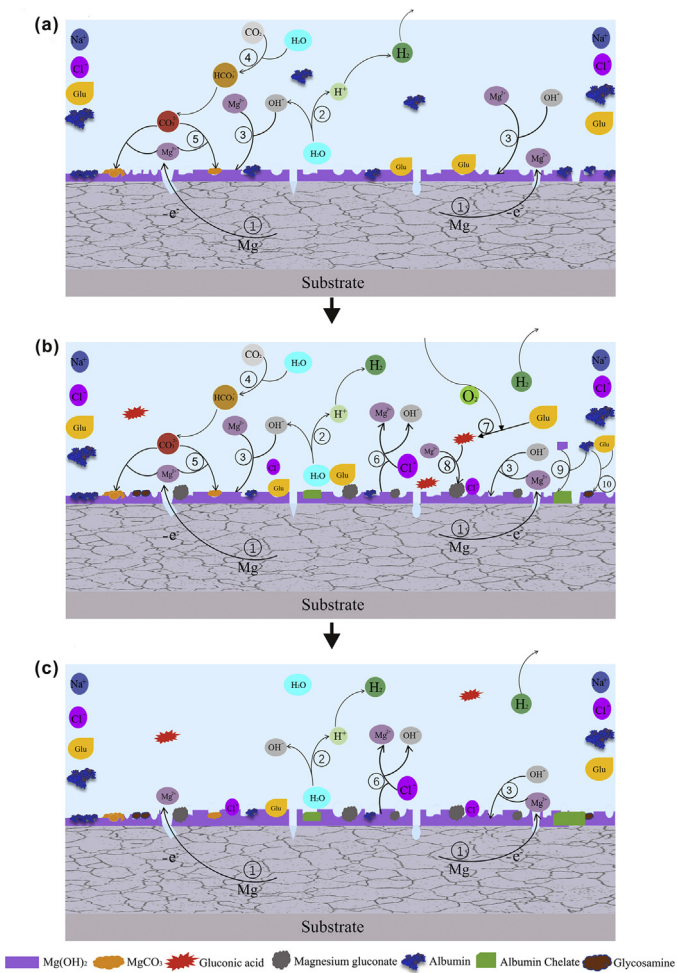


Fig. 15. Schematic diagram of the degradation mechanisms of pure Mg in: (a) NaCl solution and (b) NaCl and glucose solution [96]. (Reproduced with permission of Ref [96]. Copyright of © 2020 Elsevier).

and protein (0.1 g/L and 10 g/L) on Mg corrosion were also investigated. The results showed that low concentration glucose or protein inhibited the corrosion of Mg, and high concentration of glucose or protein promoted its degradation. The degradation mechanism of Mg under the influence of glucose and protein is shown in Fig. 15.

4.4. Coupling effect of polypeptide and heparin or protein

Wang et al. [97] found that the mixture of silk fibroin, heparin and (Gly-Arg-Glu-Asp-Val-Tyr) peptide could be fixed on the surface of HF-pretreated Mg alloy through a “double-sided tape” polydopamine layer for improving the corrosion resistance, blood compatibility, and endothelialization. Wu et al. [98] employed alkali-heat treatment and silane treatment as the pre-treatment for Mg-Zn-Y-Nd alloy to improve its corrosion resistance. The Arg-Glu-Asp-Val (REDV) peptide with anti-CD34 were modified on sample surface for further improving the surface endothelialization. Moreover, for anticoagulation and anti-inflammatory requirements, heparin was also fixed in the coating. The results showed that the composite surface achieved multiple functions, including anti-corrosion properties, promotion of endothelialization, and inhibition of platelet/macrophage adhesion.

5. Influence of glucose on microbially induced corrosion

During the long-term immersion experiments in simulated body fluids, in some case, it was found that the media pH decreases. Li et al. [99] recently reported that glucose promoted the microbial entry and the degradation of Mg-Li-Ca implants. The results showed when Mg-1Li-1Ca alloy was soaked in Hanks’ solution, the pH value of the solution decreased to about 5.0 (Fig. 16). Such a low pH value is related to the bacterial activity in the medium. Besides, the research indicates that a renewal solution containing gentamicin may be beneficial to eradicate bacterial adhesion and growth. During the immersion period, the degradation behavior of the Mg-1Li-1Ca alloy by microorganisms behaves abnormally. For Mg-1Li-1Ca alloy, glucose promotes microbial activity, which leads to the fast degradation of Mg-1Li-1Ca alloy and the deterioration of mechanical properties.

Gnedenkov et al. [100] found that during the initial soaking stage of MA8 Mg alloy, lactic acid formed by microbial growth and bacterial metabolism under non sterile conditions improved the electrochemical activity of the samples. At present, microbial corrosion of bioorganic medical materials is also receiving attraction. Therefore, when studying the biomedical process of Mg alloy, whether the microbial cor-

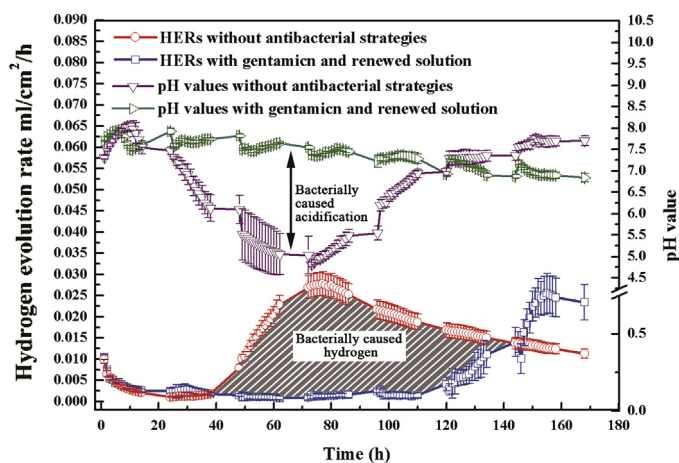


Fig. 16. Hydrogen evolution rate (HER) and pH value of the Mg-1Li-1Ca during immersion in Hanks' solution without an antibacterial strategy and daily renewal of gentamicin [99]. (Reproduced with permission of Ref [99]. Copyright of © 2020 Elsevier).

rosion exists at the application location for Mg alloy should also be considered.

6. Influence of bioorganic molecules on corrosion protection

Surface modification is a main strategy to obtain an enhancement in corrosion resistance of Mg alloys for biomedical applications [101]. Many surface treatment technologies have been employed for Mg alloys, including micro arc oxidation [102], organic coating [103–107], and chemical conversion treatment [108]. Meanwhile, organic small molecules were introduced during surface treatment process. The relevant results were summarized in the following sections.

6.1. Influence of glucose on the formation of Ca-P coating strategy

Ca-P coating is applied on the surface of Mg alloys to improve their corrosion resistance and biocompatibility, which extends the service life of Mg implants and stimulates bone regeneration [109–111]. Ca-P coating has high osteoconduction and low toxicity in physiological environments [112–116]. Some researchers employed EDTA [117], glucose [118], DNA [119,120] and amino acids [121,122] as inducers to obtain Ca-P coatings with better properties.

Li et al. [118] successfully prepared a composite coating containing a sandwich of crystalline Ca-P and $Mg(OH)_2$ on pure Mg by hydrothermal deposition in an alkaline solution with glucose. The calcium phosphate coating, consists of anhydrous calcium hydrogen phosphate, calcium-deficient hydroxyapatite (HA, $Ca_{10}(PO_4)_6(OH)_2$) and HA, enhanced the corrosion resistance of pure Mg. The filming mechanism is shown in the Fig. 17. Wen et al. [123] also used glucose to induce Ca-P coating.

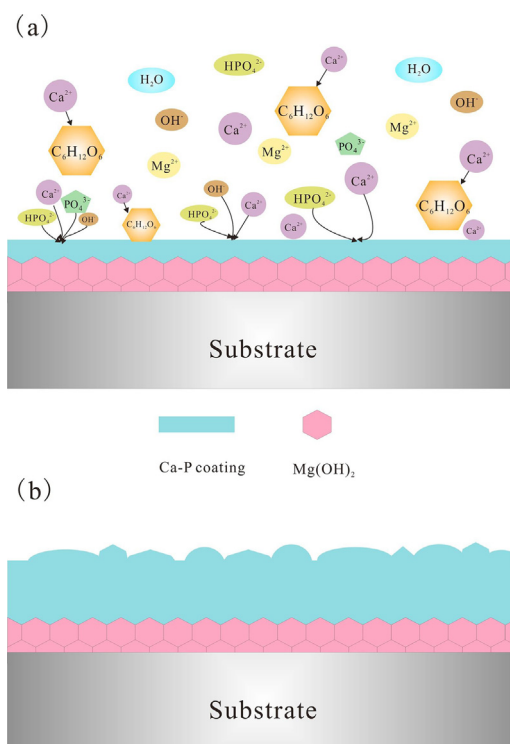


Fig. 17. Glucose induces the membrane-forming mechanism of Ca-P coating [118]. (Reproduced with permission of Ref [118]. Copyright of © 2019 Elsevier).

6.2. Influence of amino acids on the formation of Ca-P coating

Not only glucose, but also amino acids can induce calcium-phosphorus coating. Fan et al. [121] reported that the L-cysteine-induced Ca-P coating was fabricated on Mg alloy AZ31 in a water bath at 60 °C. The results pointed out that the existence of L-cysteine increased the coating thickness due to the complexation of the carboxyl and mercapto groups of L-cysteine with Ca^{2+} . Thus, the L-cysteine-induced Ca-P coating has better anti-corrosion property.

Wang et al. [122] prepared three kinds of amino acid induced Ca-P coatings ($Ca-P_{Phe}$, $Ca-P_{Met}$ and $Ca-P_{Asn}$). The thickness of Ca-P coating, $Ca-P_{Phe}$ coating, $Ca-P_{Met}$ coating and $Ca-P_{Asn}$ coating were (3.470 ± 0.47) , (6.06 ± 0.77) , (7.63 ± 0.70) and (8.231 ± 1.37) μm , respectively (Fig. 18). The main phases of the coating are $CaHPO_4$ and HA. Electrochemical tests show that the amino acid-induced calcium-phosphorus coating improves its anti-corrosion properties. Among them, $Ca-P_{Asn}$ coating has the highest corrosion resistance (Fig. 18). This is mainly due to the inhibition of amino acid molecules and the chemical adsorption on the AZ31 surface. The adsorption of amino acids is mainly realized by the coupling of lone pair electrons of N atom with the Mg alloy surface. The carboxyl group combines with Mg^{2+} through the O atom in the carbonyl group. Furthermore, the heteroatoms in amino acids can share their lone pair electrons with the vacancy molecular orbital of Mg alloy.

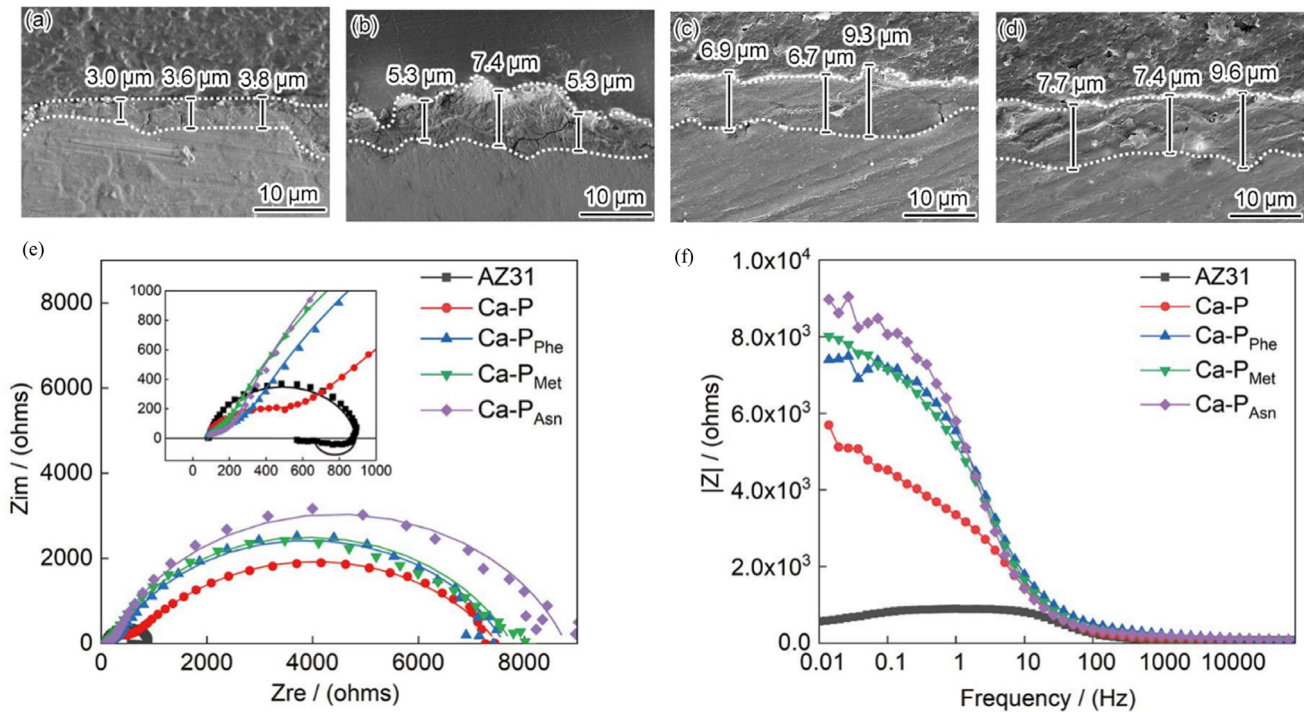


Fig. 18. Cross-sectional morphologies of Ca-P coating (a), Ca-P_{Phe} coating (b), Ca-P_{Met} coating (c), and Ca-P_{Asn} coating (d) on AZ31 Mg alloy surface; Nyquist (e) and bode (f) curves of AZ31 Mg alloy, with Ca-P coating, Ca-P_{Phe} coating, Ca-P_{Met} coating, and Ca-P_{Asn} coating [122]. (Reproduced with permission of Ref [122]. Copyright of © 2021 Science Press).

Table 3

Influence of adding several amino acids to the sol-gel coating on the corrosion resistance of AZ91.

Coating composition	Amino acids	Other additives	Corrosion resistance	Refs.
TEOS+MTES	L-alanine(0.1 wt.%) L-glutamine(0.5 wt.%) L-methionine(1.0 wt.%) L-aspartic acid(0.5 wt.%)	Null	Corrosion resistance: L-aspartic acid > L-methionine > L-glutamine > L-alanine	[92]
TEOS+TEVS	Cysteine Serine Alanine Arginine	TiO ₂	The improvement order of four amino acids on the coating performance is cysteine > serine > alanine > arginine. In addition, adding 0.5 wt.% cysteine+1.0 wt.% TiO ₂ nanoparticles into the coating containing amino acids can enhance the corrosion resistance of the coating significantly.	[126]
TEOS+MTES	L-glutamine L-methionine L-alanine	Montmorillonite Nanoparticles, Na ⁺	Adding 0.5 wt.% Na ⁺ and methionine to montmorillonite nanoparticles can lead to an improved corrosion resistance of the coating, showing a synergistic effect.	[127]

6.3. Influence of amino acids on the corrosion inhibition

Sol-gel coatings display good chemical stability, oxidation and corrosion resistance to metals [124,125]. Amino acids, as a green corrosion inhibitor, have been added into sol gel coating to fabricate the hybrid positive anti-corrosion coating Table 3. summarized the related research works.

Mei et al. [46] explored the effects of 24 amino acids on the degradation of pure Mg and Mg-0.8Ca (Table 4). It can be seen that the tested amino acids have a positive effect on the degradation resistance of pure Mg in most cases.

Part of the tested amino acid compounds have shown good inhibitory ability. Their molecular structure, concentration, used corrosive media, surface properties have an impact on the inhibitory ability of these compounds. Recent research fo-

cuses on the synthesis of new derivatives of amino acids with higher corrosion inhibition efficiency [91].

Ma et al. [128] have shown that Schiff bases inhibited the corrosion of Mg-Zn-Y-Nd in normal saline. This experiment creatively explained the influence of amino acid coupling of glucose on Mg corrosion, which not only brings a step closer to uncover the mystery of the degradation mechanism of biomedical Mg alloy in human body, but also provides a new idea for future researchers to explore the effect of interaction between different substances on the corrosion of Mg alloy.

Adding a small amount of Zn(NO₃)₂ to pure amino acids can greatly improve their inhibition efficiency. Zhang et al. [129] chose 0.05 wt.% NaCl as the corrosive solution. The results showed that the combination of L-Phe-and Zn(NO₃)₂

Table 4
Influence of individual and groups of amino acids on the degradation of Mg-0.8Ca and CP Mg [46].

Amino acid	Concentration/M	Medium	Mg-0.8Ca	CP Mg
Alanine	8.53×10^{-4}	0.9%NaCl	Accelerated	Accelerated
Serine	1.90×10^{-4}	0.9%NaCl	Accelerated	Decelerated
Aspartic	9.01×10^{-5}	0.9%NaCl	Decelerated	Decelerated
Proline	4.95×10^{-4}	0.9%NaCl	Accelerated	Accelerated
Glutamic	1.90×10^{-4}	0.9%NaCl	Accelerated	Accelerated
Cysteine	4.13×10^{-4}	0.9%NaCl	Accelerated	Decelerated
Glycine	7.19×10^{-4}	0.9%NaCl	Accelerated	Decelerated
Asparagine	1.00×10^{-4}	0.9%NaCl	Accelerated	Decelerated
Leucine	3.96×10^{-4}	0.9%NaCl	Accelerated	Decelerated
Isoleucine	3.20×10^{-4}	0.9%NaCl	Accelerated	Decelerated
Methionine	1.01×10^{-4}	0.9%NaCl	Accelerated	Decelerated
Arginine	2.07×10^{-4}	0.9%NaCl	Accelerated	Accelerated
Histidine	2.45×10^{-4}	0.9%NaCl	Accelerated	Decelerated
Valine	3.59×10^{-4}	0.9%NaCl	Accelerated	Accelerated
Tryptophan	1.47×10^{-4}	0.9%NaCl	Accelerated	Accelerated
Threonine	2.69×10^{-4}	0.9%NaCl	Accelerated	Accelerated
Phenylalanine	2.42×10^{-4}	0.9%NaCl	Accelerated	Decelerated
Glutamine	7.25×10^{-4}	0.9%NaCl	Accelerated	Accelerated
Lysine	3.97×10^{-4}	0.9%NaCl	Accelerated	Accelerated
Tyrosine	1.38×10^{-4}	0.9%NaCl	Accelerated	Decelerated
All above listed vitamins tested together		0.9%NaCl	Accelerated	Decelerated
Ornithine	1.06×10^{-4}	SBF	Decelerated	Decelerated
α -Aminobutyric acid	1.94×10^{-5}	0.9%NaCl	Accelerated	Accelerated
Taurine	1.68×10^{-4}	0.9%NaCl	Accelerated	Decelerated
Cystine	9.90×10^{-5}	0.9%NaCl	Accelerated	Accelerated

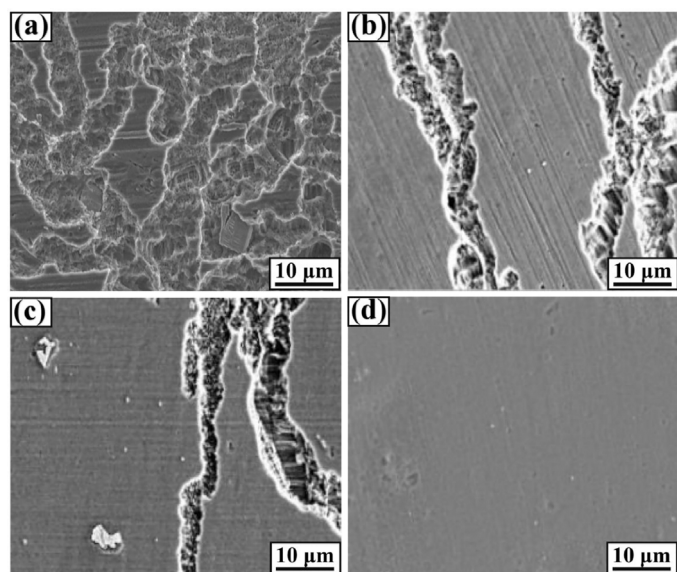


Fig. 19. SEM images of Mg alloy AZ31B after 72-h exposure to 0.05 wt.% NaCl in the absence or presence of amino acids: (a) the blank, (b) 0.07 mM $Zn(NO_3)_2$, and (c) 0.30 mM L-Phe-as well as (d) 0.30 mM L-Phe + 0.07 mM $Zn(NO_3)_2$ [129]. (Reproduced with permission of Ref [129]. Copyright of © 2021 Elsevier).

synergistically inhibited the corrosion of AZ31B in NaCl solution, which is significantly better than that of L-Phe-or $Zn(NO_3)_2$ alone, as shown in Fig. 19. The hybrid corrosion inhibitor is a mixed corrosion inhibitor with highest inhibition efficiency of 93.2%, and the anodic behavior is dominant.

6.4. Influence of vitamins C on the corrosion protection

Vitamins C, ascorbic acid, has strong activity and good antioxidant property. Biodegradable “green” ascorbic acid molecules can be used as conductive carbon source to prepare conductive corrosion-resistant coatings on Mg alloys. Thus, Takahiro et al. [130] used ascorbic acid to prepare an $Mg(OH)_2/C$ composite film on the surface of Mg alloy AZ31 using a hydrothermal method. With the increase of ascorbic acid, the thickness of the film decreases, but the carbon content increases. The film with 0.3 g of ascorbic acid has the strongest corrosion resistance.

Loperena et al. [131] produced a Ce-based conversion film on AZ91D by immersion in a solution comprising $Ce(NO_3)_3$, H_2O_2 and ascorbic acid (HAsc). It was called RCe-coating, RCe- H_2O_2 film and RCe-HAsc coating. The results showed that RCe-HAsc coating with uniform adhesion was prepared on Mg alloy AZ91D. At -0.75 V, the most adhered films were obtained through potentiostatic polarization. The corrosion resistance of RCe-HAsc coating is better than that without HAsc in the simulated physiological solution (Fig. 20). The improvement of anti-corrosion performance is related to the inhibition of insoluble chelate formation on additives.

6.5. Influence of polypeptide on the functional coating

Implant-related infection is the notorious problem in orthopedic surgery. Antimicrobial peptides (AMPS) are an important part of human immunity. Compared with traditional antibiotics, amps have little effect on the drug resistance of

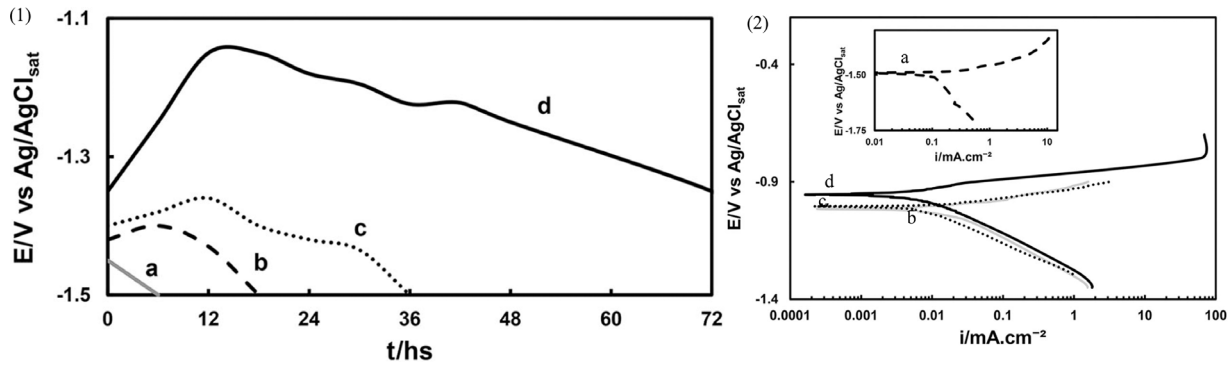


Fig. 20. (1) OCP and (2) Tafel in Ringer's solutions for: (a) AZ91D, (b) RCe-coating, and (c) RCe-H₂O₂ film and (d) RCe-HAsc coating as well [131]. (Reproduced with permission of Ref [131]. Copyright of © 2016 Elsevier).

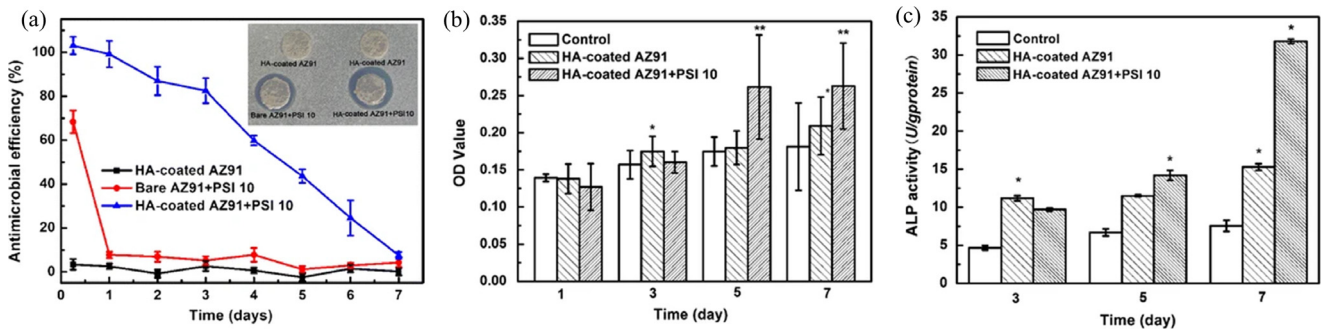


Fig. 21. (a) Antibacterial efficiency of AMP loaded Mg alloy samples against *S. aureus*, and the inset represents the inhibition zone of *S. aureus*; rBMSCs proliferation (b) and ALP analysis (c) in different extracts (* $P < 0.05$ vs. Control; ** $P < 0.01$ vs. Control.) [132] (Reproduced with permission of Ref [132]. Copyright of © 2015 Springer Link).

pathogens. Tian et al. [132] tried to deposited hydroxyapatite (HA) coating on Mg alloy and the loading of AMPS by biomimetic method. The results showed that the degradation rate for AMPS/HA coated Mg alloy is lower than that of bare HA coating. The AMP loaded HA coating showed to effective inhibition effect on the growth of *Staphylococcus aureus*. The coated sample has good biocompatibility and can promote alkaline phosphatase (ALP) activity on rat bone marrow mesenchymal stem cells (rBMSCs), as shown in Fig. 21.

Some researchers have explored the effect of Arg-Glu-Asp-Val (REDV) [133], the compound of antimicrobial peptide (AP) and silk fibroin (SF) [134], and the caerin peptide 1.9 (F3) and a modified sequence of caerin 1.1 (F1) with antibacterial activity [135] on the corrosion behavior of Mg alloys. It showed that the adding peptides led to significant improvement in the corrosion resistance and antibacterial effect of Mg alloys.

6.6. Influence of protein on the coating formation

Xiong et al. [136] prepared a bone extracellular matrix-like Ca, Sr/P silk fibroin composite films with corrosion resistance, biocompatibility and osteogenic potential on the fluoride-treated Mg-1Ca surface by spin coating technology. The composite film coated samples showed the improved corrosion resistance than that of bare Mg-Ca alloy. In addition, the cytocompatibility and ontogeny of the coating material

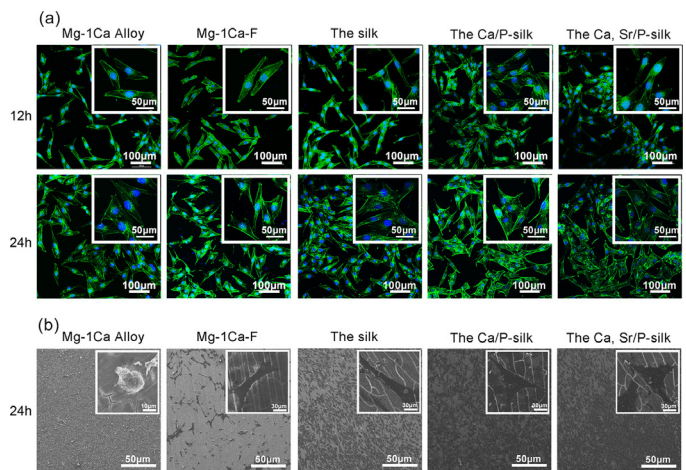


Fig. 22. (a) Actin nucleus co-staining of cells cultured for 12 and 24 h, and (b) on naked Mg-1Ca alloy, fluoride treated, pure silk membrane, Ca/P silk and Ca, Sr/P silk [136]. (Reproduced with permission of Ref [136]. Copyright of © 2018 ACS).

were significantly enhanced in the adhesion bonding, proliferation, and cytoskeleton development together with differentiation of MC3T3-E1 cells (Fig. 22).

Hou et al. [137] employed a series of analysis techniques to obtain insights on the formation and properties of the pre-formed Mefp-1 film on Mg-1.0 Ca. The results showed that

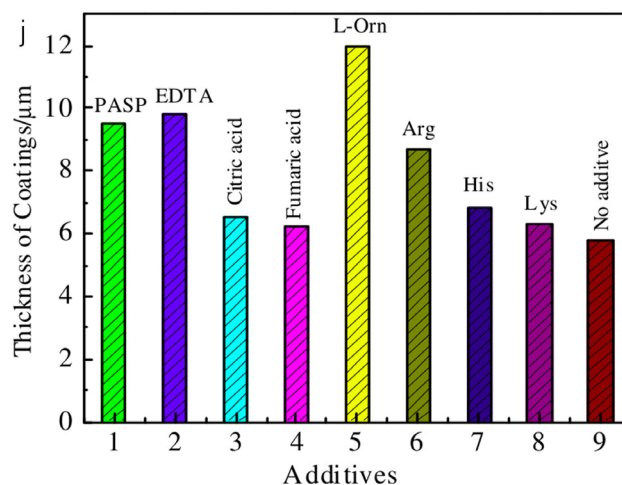
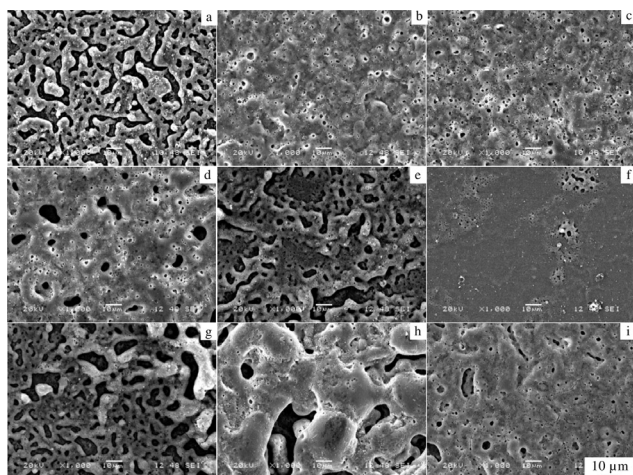


Fig. 23. SEM morphologies of anodizing film surface of Mg alloy with different additions: (a) no additive, (b) L-Orn, (c) EDTA, (d) Arg, (e) Lys, (f) His, (g) fumaric acid, (h) citric acid, and (i) PASP; and (j) thicknesses of anodizing coatings [140]. (Reproduced with permission of Ref [140]. Copyright of © 2017 Elsevier).

the Mefp-1 film preformed at pH 4.6 showed a network structure, while it was tighter at pH 8.5. The *in-situ* scanning results showed that the Mefp-1 film formed under the two pH conditions retard the localized corrosion of Mg-1.0 Ca alloy markedly.

Rahman et al. [138] employed bombyx mori silk to prepare a biomimetic silk coating on anodized Mg surface. Compared with the bare anodized samples, the decay rate of the silk coated anodized alloys in terms of hydrogen production and weight loss significantly reduced, indicating that the optimized biomimetic silk coated Mg surface shows the best corrosion performance. The cytotoxicity test results verified that the cytotoxicity of silk coated alloys is inferior to that of bare Mg and anodized Mg oxide samples.

Wang et al. [139] prepared a sodium montmorillonite (MMT)/ BSA composite coating on AZ31 by hydrothermal synthesis and immersion method. The results showed that MMT-BSA coating has good anti-corrosion property and biocompatibility in comparison to that of the naked AZ31 alloy. The MMT-BSA coated AZ31 implant hold its structural integrity, and experienced slight degradation within 120 days after implantation. No obvious toxic damage to organs and tissues was detected.

6.7. Influence of glucose and amino acids on the formation of MAO

MAO is a modified ceramic coating with substrate metal oxides and electrolyte components grown on the surface of Al, Mg, Ti and other valve metals, which has excellent anti-corrosion and anti-wear properties. Gou et al. [140] added amino acid organic additives to the basic electrolyte of NaOH + Na₂SiO₃ to anodize AZ31 alloy. The study involved the effects of amino acid organic additives (L-arginine, ethylenediamine tetraacetic acid (EDTA), L-Ornithine acetate, L-lysinehistidine, polyaspartic acid, fumaric acid, citric acid) on the anodization process, thickness, surface morphology

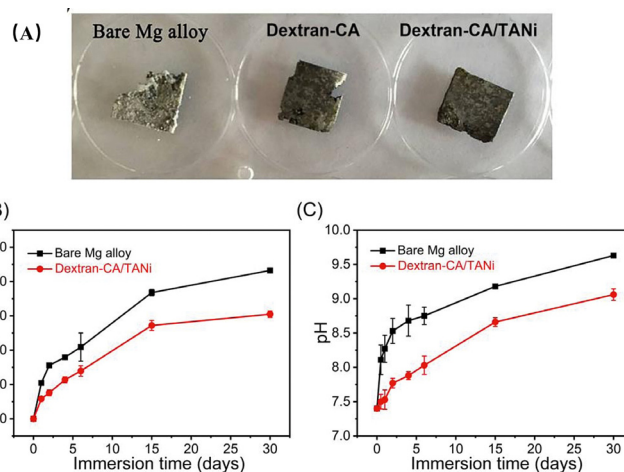


Fig. 24. (A) Digital photos of test samples after being immersed in SBF for 30 days. The change of (B) Mg²⁺ concentration and (C) media pH during the immersion period [141]. (Reproduced with permission of Ref [141]. Copyright of © 2020 Elsevier).

(Fig. 23), and microstructure as well as corrosion performance of the anodized films. The thickness of the anodic oxide film obtained before and after adding organic additives is shown in Fig. 23. It could be found that organic additives changed the thickness of the oxide film. The results showed that EDTA and L-ornithine acetate significantly increased the breakdown voltage of anodizing, playing an obvious arc suppression role, and greatly improving the thickness, compactness and degradation resistance of the oxide film. Organic additives mainly affect the anodizing process of Mg alloy and the properties of oxide film through the comprehensive effects of corrosion inhibition, arc suppression and surfactant.

6.8. Influence of other bioorganic molecules on the coating

In addition to abovementioned proteins, monosaccharides, amino acids and vitamins, many other organic substances be-

long to biological related organic molecules. They usually exist in specific parts and have specific functions and also show a positive impact on the protective coating of Mg alloy.

Li et al. [141] fabricated a hybrid coating using biocompatible dextran caffeic acid (dextran CA) and electroactive tetra aniline (TaNi) for improving the cell compatibility and anti-corrosion property of Mg alloys. The results showed that the degradation rate of dextran Ca/TaNi coated Mg alloy was significantly reduced and the cell compatibility was improved (Fig. 24). Du et al. [142] found that Mg mgoznonrs-sulfate/lysozyme (DS/Lys) coating synthesized by magnesium oxide coating, zinc oxide nanorods (znorrs) and dextran sodium (DS/Lys) facilitated the improvement in corrosion resistance, blood compatibility and antibacterial activity of Mg alloys.

7. Summary and outlooks

This review summarized the related works about the influence of biomolecules on the corrosion and protection of Mg alloys for biomedical applications. The extensive applications of Mg-based materials in biomedical field and the control of degradation rate cannot be separated from the exploration of corrosion mechanisms, especially the influence of organic matters on their corrosion behavior. Regarding the future work, the research on the influence of biomolecules on the corrosion behavior and corrosion protection of Mg alloys should be emphasized in the following aspects:

- (1) Bioorganic molecules (glucose, amino acids and protein) play a crucial role in the degradation, biomineralization and surface modification of degradable metals. Their influence cannot be ignored during the extremely complex micro-environment in human body. Further investigation remains necessary from multifactor coupling perspective, including materials, chemistry and mechanical as well as biomedical interdisciplinary study.
- (2) The research on the biocorrosion behavior of Mg alloys aims to achieve their practical applications. It is necessary to set specific experimental conditions in combination with the specific service environment to investigate the corrosion mechanism of Mg alloys coupled with organic molecules and other components under specific conditions (flow rate of corrosion medium, scouring force and renewal frequency, etc.). A testing standard for *in vitro* degradation of degradable metals is expected to be proposed by the global scientists.
- (3) Current corrosion characterization is limited for the insight into understanding the degradation mechanisms of biomedical metals. Novel approaches to explore the corrosion mechanisms of Mg are expected to be developed. The data not only comes from the experimental methods under simulated human environment, but also originates from the computational simulation methods.
- (4) Small bioorganic molecules increase the thickness, compactness and adhesion bonding of the coatings, such as Ca-P coating and MAO coating, with an improved cor-

rosion resistance of Mg alloys. However, there still exists a gap between the actual and required degradation life of Mg alloys. Further research is needed to enhance the corrosion resistance of Mg alloys with the assistance of those functional coatings.

Declaration of Competing Interest

The authors declare that they have no known competing financial interests or personal relationships that could have appeared to influence the work reported in this paper.

Acknowledgments

This work was supported by National Natural Science Foundation of China (Grant No. 52071191) and Open Foundation of Hubei Key Laboratory of Advanced Technology for Automotive Components (No. XDQCKF2021006). Thanks to the task force team: Xue-Mei Wang, Yang Shao, Pu-sheng Sui, Ai-Meng Zhang, Ze-Song Wei and other students to the thesis writing and photo production help.

References

- [1] A.A. Luo, J. Magnes. Alloy. 1 (2013) 2–22.
- [2] F. Witte, N. Hort, C. Vogt, S. Cohen, K.U. Kainer, R. Willumeit, F. Feyerabend, Curr. Opin. Solid. State Mater. 12 (2008) 63–72.
- [3] D. Zhao, F. Witte, F. Lu, J. Wang, J. Li, L. Qin, Biomaterials 112 (2017) 287–302.
- [4] A. Mohamed, A.M. El-Aziz, H.G. Breitingner, J. Magnes. Alloy. 7 (2019) 249–257.
- [5] R.C. Zeng, L.Y. Cui, W. Ke, Acta Metall. Sin. 54 (2018) 1215–1235.
- [6] J.F. Song, J. She, D.L. Chen, F.S. Pan, J. Magnes. Alloy. 8 (2020) 1–41.
- [7] Z. Li, X. Gu, S. Lou, Y. Zheng, Biomaterials 29 (2008) 1329–1344.
- [8] J.L. Wang, J.K. Xu, C. Hopkins, D.H. Chow, L. Qin, Adv. Sci. 7 (2020) 1902443.
- [9] M. Esmaily, J.E. Svensson, S. Fajardo, N. Birbilis, G.S. Frankel, S. Virtanen, R. Arrabal, S. Thomas, L.G. Johansson, Prog. Mater. Sci. 89 (2017) 92–193.
- [10] T.F. Xi, L.N. Wei, J. Liu, X.L. Liu, Z. Zhen, Y.F. Zheng, Acta Metall. Sin. 53 (2017) 1153–1167.
- [11] C.L. Liu, Y.J. Wang, R.C. Zeng, X.M. Zhang, W.J. Huang, P.K. Chu, Corros. Sci. 52 (2010) 3341–3347.
- [12] X. Li, X. Liu, S. Wu, K.W.K. Yeung, Y. Zheng, P.K. Chu, Acta Biomater. 45 (2016) 2–30.
- [13] R.C. Zeng, L. Sun, Y.F. Zheng, H.Z. Cui, E.H. Han, Corros. Sci. 79 (2014) 69–82.
- [14] R. Zeng, W. Dietzel, F. Witte, N. Hort, C. Blawert, Adv. Eng. Mater. 10 (2008) 3–14.
- [15] Y. Chen, Z. Xu, C. Smith, J. Sankar, Acta Biomater. 10 (2014) 4561–4573.
- [16] J. Wu, D. Zhao, J.M. Ohodnicki, B. Lee, A. Roy, R. Yao, S. Chen, Z. Dong, W.R. Heineman, P.N. Kumta, ACS Biomater. Sci. Eng. 4 (2018) 919–932.
- [17] H. Zhou, B. Liang, H.T. Jiang, Z.L. Deng, K.X. Yu, J. Magnes. Alloy. 9 (2021) 779–804.
- [18] D.H.K. Chow, J. Wang, P. Wan, L. Zheng, M.T.Y. Ong, L. Huang, W. Tong, L. Tan, K. Yang, L. Qin, Bioact. Mater. 6 (2021) 4176–4185.
- [19] R. Wu, Y. Li, M. Shen, X. Yang, L. Zhang, X. Ke, G. Yang, C. Gao, Z. Gou, S. Xu, Bioact. Mater. 6 (2021) 1242–1254.
- [20] L.Y. Cui, Y. Hu, R.C. Zeng, Y.X. Yang, D.D. Sun, S.Q. Li, F. Zhang, E.H. Han, J. Mater. Sci. Technol. 33 (2017) 971–986.

- [21] F. Witte, *Acta. Biomater.* 6 (2010) 1680–1692.
- [22] J. Kuhlmann, I. Bartsch, E. Willbold, S. Schuchardt, O. Holz, N. Hort, D. Hoeche, W.R. Heineman, F. Witte, *Acta. Biomater.* 9 (2013) 8714–8721.
- [23] D.L. Zhao, T.T. Wang, J. Kuhlmann, Z.Y. Dong, S.N. Chen, M. Joshi, P. Salunke, V.N. Shanov, D.H. Hong, P.N. Kumta, W.R. Heineman, *Acta Biomater.* 36 (2016) 361–368.
- [24] G.Y. Yuan, J.L. Niu, *Acta. Metall. Sin.* 53 (2017) 1168–1180.
- [25] R.C. Zeng, Y. Hu, S.K. Guan, H.Z. Cui, E.H. Han, *Corros. Sci.* 86 (2014) 171–182.
- [26] A. Yamamoto, S. Hiromoto, *Mater. Sci. Eng. C* 29 (2009) 1559–1568.
- [27] Y. Xin, K. Huo, H. Tao, G. Tang, P.K. Chu, *Acta. Biomater.* 4 (2008) 2008–2015.
- [28] Y. Jang, B. Collins, J. Sankar, Y. Yun, *Acta Biomater.* 9 (2013) 8761–8770.
- [29] G.E. Novikova, *Prot. Met. Phys. Chem.* 47 (2011) 372–380.
- [30] R. Zeng, L. Liu, S. Li, Y. Zou, F. Zhang, Y. Yang, H. Cui, E.H. Han, *Acta Metall. Sin. Engl.* 26 (2013) 681–686.
- [31] R. Zeng, Z. Lan, L. Kong, Y. Huang, H. Cui, *Surf. Coat. Tech.* 205 (2011) 3347–3355.
- [32] Y. Liu, Y.F. Zheng, X.H. Chen, J.A. Yang, H.B. Pan, D.F. Chen, L.N. Wang, J.L. Zhang, D.H. Zhu, S.L. Wu, K.W.K. Yeung, R.C. Zeng, Y. Han, S.K. Guan, *Adv. Funct. Mater.* 29 (2019) 1805402.
- [33] S. Höhn, S. Virtanen, A.R. Boccaccini, *Appl. Surf. Sci.* 464 (2019) 212–219.
- [34] B. Neirinck, F. Singer, A. Braem, S. Virtanen, J. Vleugels, *Key Eng. Mater.* 654 (2015) 139–143.
- [35] Z.Q. Zhang, L. Wang, M.Q. Zeng, R.C. Zeng, M.B. Kannan, C.G. Lin, Y.F. Zheng, *Bioact. Mater.* 5 (2020) 398–409.
- [36] Y. Song, D. Shan, E.H. Han, *J. Mater. Sci. Technol.* 33 (2017) 954–960.
- [37] D.W. Wang, Y. Cao, H. Qiu, Z.G. Bi, *J. Biomed. Mater. Res. A* 99A (2011) 166–172.
- [38] R.C. Zeng, X.T. Li, S.Q. Li, F. Zhang, E.H. Han, *Sci. Rep.* 5 (2015) 13026.
- [39] L.Y. Cui, X.T. Li, R.C. Zeng, S.Q. Li, E.H. Han, L. Song, *Front. Mater. Sci.* 11 (2017) 284–295.
- [40] L.Y. Li, B. Liu, R.C. Zeng, S.Q. Li, F. Zhang, Y.H. Zou, H.G. Jiang, X.B. Chen, S.K. Guan, Q.Y. Liu, *Front. Mater. Sci.* 12 (2018) 184–197.
- [41] Y. Liu, Z. Liu, L. Liu, H. Xue, Q. Wang, D. Zhang, *Adv. Eng. Mater.* 23 (2021) 2001451.
- [42] D.B. Pokharel, W. Liping, J. Dong, X. Wei, I.I.N. Etim, D.B. Subedi, A.J. Umoh, W. Ke, *J. Mater. Sci. Technol.* 66 (2021) 202–212.
- [43] Y. Wang, B.H. Ding, S.Y. Gao, X.B. Chen, R.C. Zeng, L.Y. Cui, S.J. Li, S.Q. Li, Y.H. Zou, E.H. Han, S.K. Guan, Q.Y. Liu, *Mater. Sci. Eng. C* 105 (2019) 110042.
- [44] Y. Wang, L.Y. Cui, R.C. Zeng, S.Q. Li, Y.H. Zou, E.H. Han, *Materials* 10 (2017) 725 (Basel).
- [45] D.B. Pokharel, L. Wu, J. Dong, A.P. Yadav, D.B. Subedi, M. Dhakal, L. Zha, X. Mu, A.J. Umoh, W. Ke, *J. Mater. Sci. Technol.* 81 (2021) 97–107.
- [46] D. Mei, S.V. Lamaka, C. Feiler, M.L. Zheludkevich, *Corros. Sci.* 153 (2019) 258–271.
- [47] E.P. Silva, R.H. Buzolin, F. Marques, F. Soldera, U. Alfaro, H.C. Pinto, *J. Magnes. Alloy.* 9 (2021) 995–1006.
- [48] L. Li, T. Wang, Y. Wang, C.C. Zhang, H. Lv, H. Lin, W.B. Yu, C.J. Huang, *J. Magnes. Alloy.* 8 (2020) 499–509.
- [49] Z. Zhang, G. Wu, A. Atrens, W. Ding, *J. Magnes. Alloy.* 8 (2020) 301–317.
- [50] L. Li, D.J. Li, X.Q. Zeng, A.A. Luo, B. Hu, A.K. Sachdev, L.L. Gu, W.J. Ding, *J. Magnes. Alloy.* 8 (2020) 565–577.
- [51] E. Karakulak, *J. Magnes. Alloy.* 7 (2019) 355–369.
- [52] W. Pachla, S. Przybysz, A. Jarzebska, M. Bieda, K. Sztwiertnia, M. Kulczyk, J. Skiba, *Bioact. Mater.* 6 (2021) 26–44.
- [53] L. Zhong, Y. Wang, Y. Dou, *J. Magnes. Alloy.* 7 (2019) 637–647.
- [54] K. Guan, R. Ma, J. Zhang, R. Wu, Q. Yang, J. Meng, *J. Magnes. Alloy.* 9 (2021) 1098–1109.
- [55] M. Janbozorgi, K.K. Taheri, A.K. Taheri, *J. Magnes. Alloy.* 7 (2019) 80–89.
- [56] J. Li, A. Zhang, H. Pan, Y. Ren, Z. Zeng, Q. Huang, C. Yang, L. Ma, G. Qin, *J. Magnes. Alloy.* 9 (2021) 1297–1303.
- [57] V.E. Bazhenov, A.V. Li, A.A. Komissarov, A.V. Koltygin, S.A. Tavalzhanskii, V.A. Bautin, O.O. Voropaeva, A.M. Mukhametshina, A.A. Tokar, *J. Magnes. Alloy.* 9 (2021) 1428–1442.
- [58] Y.K. Li, M. Zha, J. Rong, H.I. Jia, Z.Z. Jin, H.M. Zhang, P.K. Ma, H.Xu, T.T. Feng, H.Y. Wang, *J. Mater. Sci. Technol.* 88 (2021) 215–225.
- [59] B.N. Du, Z.Y. Hu, J.L. Wang, L.Y. Sheng, H. Zhao, Y.F. Zheng, T.F. Xi, *Bioact. Mater.* 5 (2020) 219–227.
- [60] C.M. Wu, P.W. Peng, H.H. Chou, K.L. Ou, E. Sugiato, C.M. Liu, C.F. Huang, *J. Alloy. Compd.* 735 (2018) 2604–2610.
- [61] R.C. Zeng, W. Dietzel, R. Zettler, W.M. Gan, X.X. Sun, T. Nonferr, *Metal. Soc.* 24 (2014) 3060–3069.
- [62] J. Gonzalez, S.V. Lamaka, D. Mei, N. Scharnagl, F. Feyerabend, M.L. Zheludkevich, R. Willumeit-Römer, *Adv. Healthc. Mater.* 10 (2021) 2100053.
- [63] R. Rettig, S. Virtanen, *J. Biomed. Mater. Res. A* 88 (2009) 359–369.
- [64] L. Wang, T. Shinohara, B.P. Zhang, *J. Alloy. Compd.* 496 (2010) 500–507.
- [65] M.G. Acharya, A.N. Shetty, *J. Magnes. Alloy.* 7 (2019) 98–112.
- [66] F.E. Heakal, A.M. Fekry, M.Z. Fatayerji, *J. Appl. Electrochem.* 39 (2008) 583–591.
- [67] M.C. Merino, A. Pardo, R. Arrabal, S. Merino, P. Casajús, M. Moledano, *Corros. Sci.* 52 (2010) 1696–1704.
- [68] M.C. Zhao, M. Liu, G.L. Song, A. Atrens, *Corros. Sci.* 50 (2008) 3168–3178.
- [69] H. Altun, S. Sen, *Mater. Des.* 25 (2004) 637–643.
- [70] J. Li, Q. Jiang, H. Sun, Y. Li, *Corros. Sci.* 111 (2016) 288–301.
- [71] D. Mei, S.V. Lamaka, X. Lu, M.L. Zheludkevich, *Corros. Sci.* 171 (2020) 108722.
- [72] E.L. Silva, S.V. Lamaka, D. Mei, M.L. Zheludkevich, *ChemistryOpen* 7 (2018) 664–668.
- [73] M. Strebl, S. Virtanen, *J. Electrochem. Soc.* 166 (2018) C3001–C3009.
- [74] M.G. Strebl, M.P. Bruns, G. Schulze, S. Virtanen, *J. Electrochem. Soc.* 168 (2021) 1502.
- [75] L. Wang, T. Shinohara, B.P. Zhang, *Mater. Trans.* 50 (2009) 2563–2569.
- [76] D. Snihirova, M. Taryba, S.V. Lamaka, M.F. Montemor, *Corros. Sci.* 112 (2016) 408–417.
- [77] R. Hou, R. Willumeit-Römer, V.M. Garamus, M. Frant, J. Koll, F. Feyerabend, *ACS Appl. Mater. Interfaces* 10 (2018) 42175–42185.
- [78] J. Chen, S.M. Cramer, *J. Chromatogr. A* 1165 (2007) 67–77.
- [79] H. Noh, S.T. Yohe, E.A. Vogler, *Biomaterials* 29 (2008) 2033–2048.
- [80] L.T. Allen, M. Tosetto, I.S. Miller, D.P. O'Connor, S.C. Penney, I. Lynch, A.K. Keenan, S.R. Pennington, K.A. Dawson, W.M. Gallagher, *Biomaterials* 27 (2006) 3096–3108.
- [81] N. Aissaoui, L. Bergaoui, J. Landoulsi, J.F. Lambert, S. Boujday, *Langmuir* 28 (2012) 656–665.
- [82] I. Johnson, W. Jiang, H. Liu, *Sci. Rep.* 7 (2017) 14335.
- [83] M. Talha, Y. Ma, P. Kumar, Y. Lin, A. Singh, *Colloids Surf. B* 176 (2019) 494–506.
- [84] D. Mei, C. Wang, S.V. Lamaka, M.L. Zheludkevich, *J. Magnes. Alloy.* 9 (2021) 805–817.
- [85] H. Wang, Z. Fang, Y. Zhao, S. Yao, J. Li, J. Wang, S. Zhu, C. Niu, Y. Jia, S. Guan, *Appl. Surf. Sci.* 512 (2020) 145725.
- [86] H. Wang, H. Yuan, J. Wang, E. Zhang, M. Bai, Y. Sun, J. Wang, S. Zhu, Y. Zheng, S. Guan, *Acta. Biomater.* 129 (2021) 323–332.
- [87] R. Hou, F. Feyerabend, H. Helmholz, V.M. Garamus, R. Willumeit-Römer, *J. Magnes. Alloy.* (2021), doi:10.1016/j.jma.2021.07.021.
- [88] Z.Q. Zhang, H.Y. Wang, L. Wang, X.B. Chen, S.K. Guan, C.G. Lin, R.C. Zeng, *J. Magnes. Alloy.* (2021), doi:10.1016/j.jma.2021.04.005.
- [89] Y. Zhang, J. Cao, X. Wang, H. Liu, Y. Shao, C. Chu, F. Xue, J. Bai, *Bioact. Mater.* 7 (2022) 217–226.

- [90] X. Liu, Y. Cheng, Z. Guan, Y. Zheng, *Corros. Sci.* 170 (2020) 108661.
- [91] B. El Ibrahimy, A. Jmiai, L. Bazzi, S. El Issami, *Arab. J. Chem.* 13 (2020) 740–771.
- [92] H. Ashassi-Sorkhabi, S. Moradi-Alavian, M.D. Esrafil, A. Kazempour, *Prog. Org. Coat.* 131 (2019) 191–202.
- [93] E.E. Oguzie, Y. Li, F.H. Wang, *J. Colloid Interface Sci.* 310 (2007) 90–98.
- [94] N.O. Eddy, *J. Adv. Res.* 2 (2011) 35–47.
- [95] I. Sekine, Y. Nakahata, H. Tanabe, *Corros. Sci.* 28 (1988) 987–1001, doi:10.1016/0010-938X(88)90016-9.
- [96] W. Yan, Y.J. Lian, Z.Y. Zhang, M.Q. Zeng, Z.Q. Zhang, Z.Z. Yin, L.Y. Cui, R.C. Zeng, *Bioact. Mater.* 5 (2020) 318–333.
- [97] P. Wang, P. Xiong, J. Liu, S. Gao, T. Xi, Y. Cheng, *J. Mater. Chem. B* 6 (2018) 966–978.
- [98] Y. Wu, L. Chang, J. Li, L. Wang, S. Guan, *J. Biomater. Appl.* 35 (2020) 158–168.
- [99] L.Y. Li, Z.Z. Han, R.C. Zeng, W.C. Qi, X.F. Zhai, Y. Yang, Y.T. Lou, T. Gu, D. Xu, J.Z. Duan, *Bioact. Mater.* 5 (2020) 902–916.
- [100] A.S. Gnedenkoy, D. Mei, S.V. Lamaka, S.L. Sinebryukhov, D.V. Mashataly, I.E. Vyalyi, M.L. Zheludkevich, S.V. Gnedenkoy, *Corros. Sci.* 170 (2020) 108689.
- [101] Z.Q. Zhang, Y.X. Yang, J.A. Li, R.C. Zeng, S.K. Guan, *Bioact. Mater.* 6 (2021) 4729–4757.
- [102] C.Y. Li, X.L. Fan, L.Y. Cui, R.C. Zeng, *Corros. Sci.* 168 (2020) 108570.
- [103] L.C. Córdoba, A. Marques, M. Taryba, T. Coradin, F. Montemor, *Surf. Coat. Tech.* 341 (2018) 103–113.
- [104] L.Y. Li, L.Y. Cui, R.C. Zeng, S.Q. Li, X.B. Chen, Y. Zheng, M.B. Kannan, *Acta. Biomater.* 79 (2018) 23–36.
- [105] J.A. Li, L. Chen, X.Q. Zhang, S.K. Guan, *Mater. Sci. Eng. C* 109 (2020) 110607.
- [106] A. Samadi, R. Amini, M. Rostami, P. Kardar, M. Fedel, *Pigment. Resin Technol.* 50 (2020) 58–65.
- [107] K.H. Cheon, C. Park, M.H. Kang, I.G. Kang, M.K. Lee, H. Lee, H.E. Kim, H.D. Jung, T.S. Jang, *Bioact. Mater.* 6 (2021) 1189–1200.
- [108] P. Zhou, B. Yu, Y. Hou, G. Duan, L. Yang, B. Zhang, T. Zhang, F. Wang, *Corros. Sci.* 178 (2021) 109069.
- [109] T. Mokabber, Q. Zhou, A.I. Vakis, P. van Rijn, Y.T. Pei, *Mater. Sci. Eng. C Mater. Biol. Appl.* 100 (2019) 475–484.
- [110] E. Yilmaz, B. Cakiroglu, A. Gokce, F. Findik, H.O. Gulsoy, N. Gulsoy, O. Mutlu, M. Ozacar, *Mater. Sci. Eng. C* 101 (2019) 292–305.
- [111] P. Amaravathy, T.S.S. Kumar, *J. Magnes. Alloy.* 7 (2019) 584–596.
- [112] K. Batebi, B. Abbasi Khazaei, A. Afshar, *Surf. Coat. Tech.* 352 (2018) 522–528.
- [113] S. Singh, G. Singh, N. Bala, *Mater. Chem. Phys.* 237 (2019) 121884.
- [114] S. Cheng, W. Wang, D. Wang, B. Li, J. Zhou, D. Zhang, L. Liu, F. Peng, X. Liu, Y. Zhang, *Biomater. Sci.* 8 (2020) 3320–3333.
- [115] V. Aina, L. Bergandi, G. Lusvardi, G. Malavasi, F.E. Imrie, I.R. Gibson, G. Cerrato, D. Ghigo, *Mater. Sci. Eng. C* 33 (2013) 1132–1142.
- [116] Y. Su, K. Li, K. Guan, X. Zhu, J. Sun, *Mater. Sci. Eng. C* 95 (2019) 49–56.
- [117] L.Y. Cui, G.B. Wei, Z.Z. Han, R.C. Zeng, L. Wang, Y.H. Zou, S.Q. Li, D.K. Xu, S.K. Guan, *J. Mater. Sci. Technol.* 35 (2019) 254–265.
- [118] L.Y. Li, L.Y. Cui, B. Liu, R.C. Zeng, X.B. Chen, S.Q. Li, Z.L. Wang, E.H. Han, *Appl. Surf. Sci.* 465 (2019) 1066–1077.
- [119] P. Liu, J.M. Wang, X.T. Yu, X.B. Chen, S.Q. Li, D.C. Chen, S.K. Guan, R.C. Zeng, L.Y. Cui, *J. Magnes. Alloy.* 7 (2019) 144–154.
- [120] L.Y. Cui, L. Gao, J.C. Zhang, Z. Tang, X.L. Fan, J.C. Liu, D.C. Chen, R.C. Zeng, S.Q. Li, K.Q. Zhi, *J. Magnes. Alloy.* 9 (2021) 266–280.
- [121] X.L. Fan, C.Y. Li, Y.B. Wang, Y.F. Huo, S.Q. Li, R.C. Zeng, *J. Mater. Sci. Technol.* 49 (2020) 224–235.
- [122] X.M. Wang, Z.Z. Yin, X.T. Yu, Y.H. Zou, R.C. Zeng, *Acta. Metall. Sin.* 57 (2021) 1258–1271.
- [123] S. Wen, X. Liu, J. Ding, Y. Liu, Z. Lan, Z. Zhang, G. Chen, *Prog. Nat. Sci.* 31 (2021) 324–333.
- [124] D. Wang, G.P. Bierwagen, *Prog. Org. Coat.* 64 (2009) 327–338.
- [125] S. Nezamdoust, D. Seifzadeh, Z. Rajabalizadeh, *J. Magnes. Alloy.* 7 (2019) 419–432.
- [126] M.A. Ashraf, Z. Liu, W.X. Peng, N. Yooysefi, *Prog. Org. Coat.* 136 (2019) 105296.
- [127] H. Ashassi-Sorkhabi, S. Moradi-Alavian, R. Jafari, A. Kazempour, E. Asghari, *Mater. Chem. Phys.* 225 (2019) 298–308.
- [128] L. Ma, W. Li, S. Zhu, L. Wang, S. Guan, *Corros. Sci.* 184 (2021) 109268.
- [129] Y. Zhang, Y. Wu, N. Li, Y. Jiang, Y. Qian, L. Wang, J. Zhang, *J. Taiwan Inst. Chem. E* 121 (2021) 48–60.
- [130] T. Ishizaki, N. Kamiyama, E. Yamamoto, S. Kumagai, T. Sudare, N. Saito, *J. Electrochem. Soc.* 162 (2015) 741–743.
- [131] A.P. Loperena, I.L. Lehr, S.B. Saidman, *J. Magnes. Alloy.* 4 (2016) 278–285.
- [132] J. Tian, S. Shen, C. Zhou, X. Dang, Y. Jiao, L. Li, S. Ding, H. Li, *J. Mater. Sci. Mater. Med.* 26 (2015) 66.
- [133] L. Chen, J. Li, S. Wang, S. Zhu, C. Zhu, B. Zheng, G. Yang, S. Guan, *J. Mater. Res.* 33 (2018) 4123–4133.
- [134] W. Zhou, J. Yan, Y. Li, L. Wang, L. Jing, M. Li, S. Yu, Y. Cheng, Y. Zheng, *Biomater. Sci.* 9 (2021) 807–825.
- [135] T. Wang, G. Ni, T. Furushima, H. Diao, P. Zhang, S. Chen, C.E. Fogarty, Z. Jiang, X. Liu, H. Li, *Mater. Sci. Eng. C* 121 (2021) 111819.
- [136] P. Xiong, Z. Jia, M. Li, W. Zhou, J. Yan, Y. Wu, Y. Cheng, Y. Zheng, *ACS Biomater. Sci. Eng.* 4 (2018) 3163–3176.
- [137] R.Q. Hou, F. Zhang, P.L. Jiang, S.G. Dong, J.S. Pan, C.J. Lin, *Corros. Sci.* 164 (2020) 108309.
- [138] M. Rahman, N.K. Dutta, N.R. Choudhury, *Mater. Sci. Eng. C* 121 (2021) 111811.
- [139] J. Wang, L. Cui, Y. Ren, Y. Zou, J. Ma, C. Wang, Z. Zheng, X. Chen, R. Zeng, Y. Zheng, *J. Mater. Sci. Technol.* 47 (2020) 52–67.
- [140] Y.N. Gou, D.F. Zhang, Yi.D. Zhang, C.Y. Zhang, *Rare Metal. Mat. Eng.* 46 (2017) 1103–1109.
- [141] X. Li, H. Shi, Y. Cui, K. Pan, W. Wei, X. Liu, *Prog. Org. Coat.* 149 (2020) 105928.
- [142] M. Du, M. Peng, B. Mai, F. Hu, X. Zhang, Y. Chen, C. Wang, *Surf. Coat. Tech.* 384 (2020) 125336.